Chapter 3. OMEGA Extended Performance (EP) Laser System

3.0 INTRODUCTION

The OMEGA Extended Performance (EP) Laser System was completed in April 2008 and provides a significant enhancement to the experimental capability of LLE. It includes four NIF-scale beamlines, two of which can be compressed to short pulse (1 to 100 ps) in a grating compressor chamber. The compressed pulses can be propagated to the OMEGA target chamber or the OMEGA EP target chamber. Alternatively, all four OMEGA EP beams can be frequency converted to the third harmonic and propagated to the OMEGA EP chamber as long-pulse beams. The many combinations of beam paths, pulse widths, and wavelengths built into the OMEGA EP design greatly increase the diversity of experiments that can be performed at LLE, including short-pulse backlighting, high-energy-density physics, ultra-intense laser–matter interactions, and fast-ignition physics. It is possible to send two compressed 1053-nm pulses and two long-pulse, 351-nm pulses into the OMEGA EP target chamber on the same shot for short-pulse interactions with preformed plasmas. A Principal Investigator (PI) conducting experiments on OMEGA, which utilize the OMEGA EP short-pulse beams, must be a qualified PI on both laser facilities.

This chapter describes the OMEGA EP Laser System.[1,2] Section 3.1 provides an overview of the system. The performance specifications in the various possible configurations are given in Sec. 3.2. A more-detailed description of the system is given in Sec. 3.3, including laser sources, amplifiers, and power conditioning; the beamlines and their alignment and diagnostics systems; the pulse compression of the IR beams and the frequency conversion of the long-pulse beams; and the target chamber and experimental systems. Control systems are covered in Sec. 3.4 and operations in Sec. 3.5.

3.1 SYSTEM OVERVIEW

This section provides an overview of the OMEGA EP Laser System. The facility (Fig. 3.1) is housed in a building attached to the south side of the existing LLE building. The OMEGA EP target chamber is east of the existing OMEGA target chamber. The most significant structural feature of the building constructed for the laser system is an 83-ft-wide, 263-ft-long, one-story-high (14-ft) concrete box-beam. The first and second floors of this structure are 30-in.-thick slabs that serve as a rigid optical table. The lower floor rests on a bed of compacted gravel and is structurally independent from the building in which it is enclosed. This structural approach was based on the success of the original OMEGA facility design. It provides the high degree of vibration isolation that is necessary for precision laser operations.

The area inside the box-beam on the lower level contains the Diagnostic Bays, the Sources Bay, and two Capacitor Bays that house the laser-amplifier power conditioning system. The Sources and Laser Bays are climate controlled and operate as Class-1000 clean rooms but perform to nearly

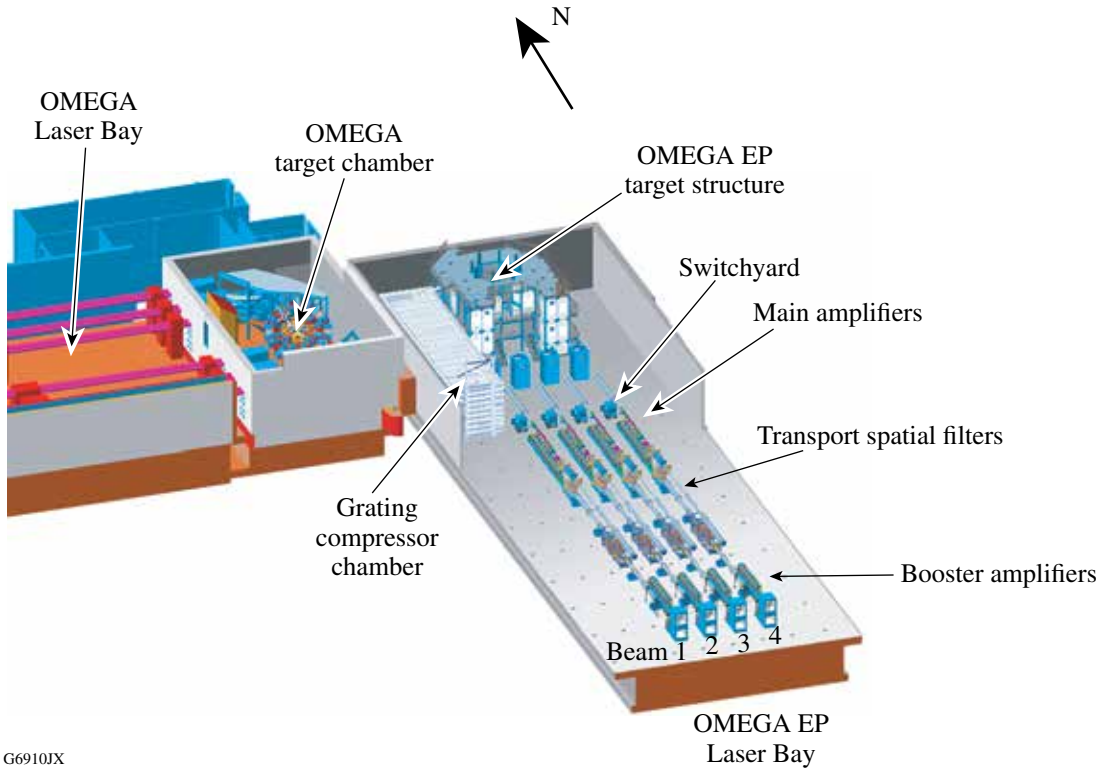

Figure 3.1
A simplified view of the OMEGA EP Laser Bay showing the four beamlines, grating compressor chamber, and target area structure relative to the OMEGA Laser System.

Class-100 conditions. A control room is provided on the second floor to the east of the Laser Bay and a viewing gallery is located at the north end of the Laser Bay.

The four laser beamlines are arranged horizontally across the floor to the south of the grating compression chamber and the target chamber and its supporting structure (Figs. 3.1 and 3.2). Beams 1 and 2 may be diverted by mirrors in the short-pulse switchyard into the grating compressor chamber and temporally compressed to short-pulse IR beams.

A schematic diagram of the main components of a beamline is shown in Fig. 3.3. The system architecture is modeled on the National Ignition Facility (NIF).[3] Each beamline is "folded" into two levels: an upper level that includes a 7-disk booster amplifier and transport spatial filter and a lower level that forms a cavity between the cavity end mirror to the south and the deformable mirror. The cavity includes an 11-disk main amplifier, a cavity spatial filter, and a plasma-electrode Pockels cell (PEPC). The deformable mirror corrects wavefront errors in the laser pulse that originate from aberrations in the optics and from prompt-induced distortion of the laser disks produced when the amplifiers fire. The PEPC is an electro-optical switch that uses polarization rotation to trap the laser pulse in the cavity, providing an additional double pass through the main amplifier to increase the gain.

G7534J1

Figure 3.2
OMEGA EP beamlines as seen from the target area structure looking south.

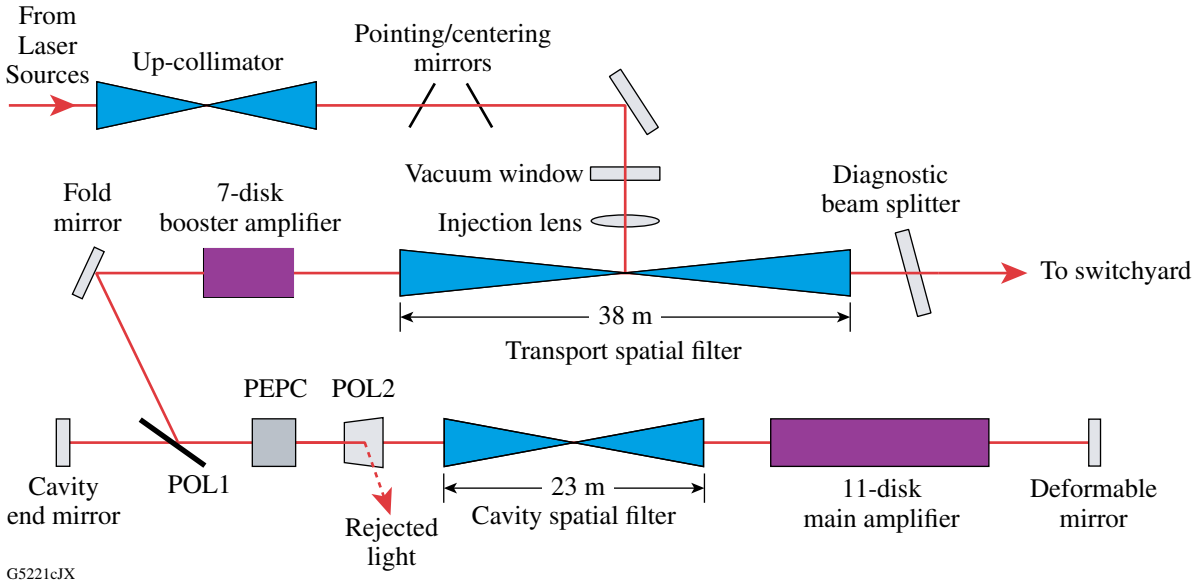

Figure 3.3
Optical components for the injection and amplification portions of an OMEGA EP beamline (PEPC: plasma-electrode Pockels cell; POL: polarizer). Beamlines 3 and 4 do not have short-pulse capability and therefore do not require POL2.

The seed laser pulse (generated in the Laser Sources Bay) is injected into the transport spatial filter via a periscope. For short-pulse experiments in either target chamber, the seed pulses of Beams 1 and/or 2 are generated as ~2.4-ns chirped pulses using optical parametric chirped-pulse amplification (OPCPA). For long-pulse UV operation, the beamlines are seeded by narrowband pulses of 100-ps to 10-ns duration and arbitrary (PI-specified) temporal waveform. The injected pulse passes through the booster amplifier and is reflected off the fold mirror to a Brewster's-angle polarizer (POL1 of Fig. 3.3) and into the main amplifier. The pulse makes two round-trips through the cavity to gain the required energy, then returns through the booster amplifier and transport spatial filter, and propagates to the switchyard. In the switchyard (Fig. 3.4), the beam is directed into the grating compressor chamber for temporal pulse compression or to frequency-conversion crystals (FCC's) for conversion to the UV. A second polarizer (POL2 of Fig. 3.3) is inserted between the PEPC and the cavity spatial filter during short-pulse operation to prevent light reflected from the target from re-entering the main amplifier.

Depending on the individual beamline and experimental conditions, the amplified pulse emerging from the transport spatial filter may take one of several paths, as shown in Fig. 3.4. For short-pulse experiments, Beam 1 and Beam 2 may be routed to the lower and upper compressor, respectively, in the grating compressor chamber, where four matched multilayer-dielectric tiled grating assemblies temporally compress the pulse. A deformable mirror after the fourth tiled grating assembly provides static wavefront correction, primarily for grating phase errors. After passing through their individual compressors, the beams can be co-aligned through a polarizing beam splitter known as the beam combiner. Beam 2 is reflected off this optic in *s* polarization while Beam 1 is transmitted in *p* polarization. The co-aligned beams are routed to one of the target chambers using the target-chamber selection mirror and focused using an *f*/1.8 off-axis parabolic mirror. While in the co-propagation alignment mode, a higher repetition rate, typically 45 min, can be obtained for 10-ps backlighting by alternating beams on successive shots. Transport from the grating compressor chamber is in an evacuated beam-transport tube connected to the target chamber being used. Alternatively, after the compressed pulses reflect off their respective deformable mirrors, the beam from the upper compressor may be directed to the OMEGA EP "backlighter" port and the beam from the lower compressor independently to the OMEGA EP "sidelighter" port. This allows targets irradiated by long-pulse, 351-nm beams to be radiographed from two orthogonal directions on the same shot and targets irradiated by the compressed, backlighter pulse to be radiographed by the sidelighter pulse. The experimental configuration flexibility is frequently used by PI's in the design of experiments; any questions regarding capabilities should be directed to the Omega Experimental User Coordinator. The variety of configurations also has schedule implications; for example, conversion of one beam from short pulse to long pulse typically involves significant work over one maintenance day. The proposed experimental configuration must be identified at the beginning of the scheduling process to enable experiments to be scheduled in an efficient sequence.

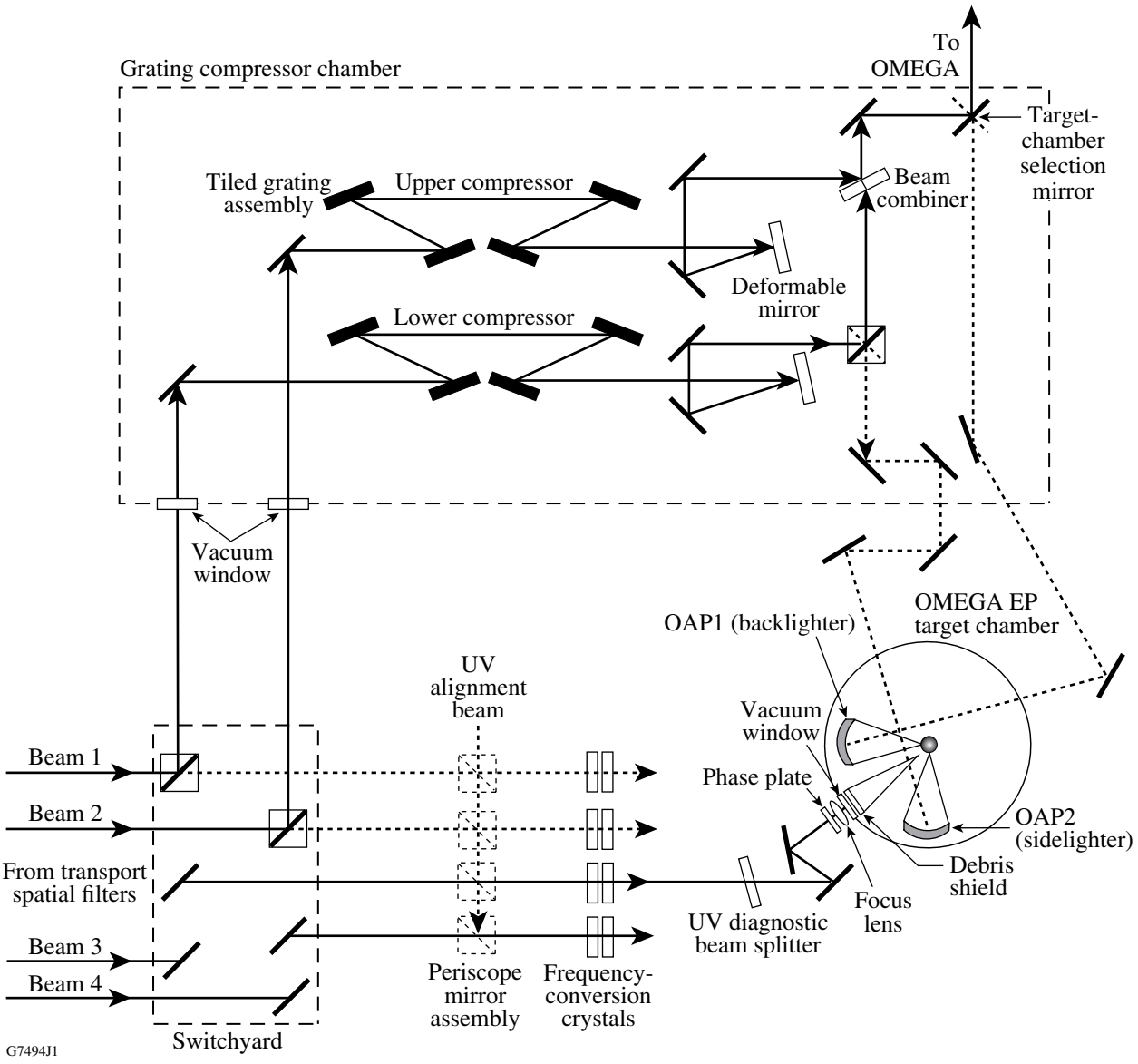

Figure 3.4
Beam paths through the switchyard, grating compressor chamber, and frequency-conversion crystals to the OMEGA and OMEGA EP target chambers. The short-pulse beams in the OMEGA EP target chamber can be focused from orthogonal directions with off-axis parabolas OAP1 and OAP2.

3.2 SYSTEM PERFORMANCE SPECIFICATIONS

The short-pulse beams can be compressed to pulse widths in the range of <1 to 100 ps. The maximum energy specifications for these beams are given in Table 3.1 for (1) a 1-ps (best-compression) beam providing the maximum on-target intensity; (2) a 10-ps beam; and (3) a co-propagated beam. For short-pulse backlighting, the pulse width and spot size depend on the requirements of the specific experiment. These design energies are not currently achievable because of the laser-damage threshold of the transport optics. LLE maintains an active log of the performance available at any given time and the Omega EP Laser Facility Manager can also be contacted if there are any questions.

The parameters in Table 3.1 depict a 2014 example of the posted energy limits of the short-pulse beams; current limits are always available on the Operations webpage. The beams are primarily limited by the laser damage-threshold of the multilayer dielectric reflection gratings. The NIF-like laser beamlines, even at the relatively short output stretched pulse length of 1.13 ns, are capable of producing >4.0 kJ of energy at the input to the compressors. The final gratings are critical because

Table 3.1: Operational Performance parameters for the 1053-nm chirped-pulse-amplification beams as of 2014. Actual performance parameters are maintained in the operations website and are slightly reduced from these values for some pulse durations.
[see https://epops.lle.rochester.edu/docs/EP_performance_envelope.pdf]

Non co-propagating short-pulse (IR) beams		Beam			
On-target energy	Pulse length	1 (current)	1 (full spec)	2 (current)	2 (full spec)
No disposable debris shield	0.7 ps	50 J	700 J	400 J	700 J
	10 ps	850 J	2600 J	1250 J	2600 J
	100 ps	1000 J	2600 J	2600 J	2600 J
With disposable debris shield	0.7 ps	50 J	50 J	50 J	50 J
	10 ps	850 J	850 J	850 J	850 J
	100 ps	1000 J	2600 J	2600 J	2600 J

Co-propagating short-pulse (IR) beams		Beam 1 on-target energy (100 ps)		
	BL 2 Pulse length	850 J to 1000 J	750 J to 800 J	≤650 J
BL2 on-target energy, no DDS	0.7 ps	300 J	300 J	350 J
	10 ps	1000 J	1250 J	1250 J
	100 ps	1500 J	1750 J	1750 J
BL2 on-target energy, with DDS	0.7 ps	50 J	50 J	50 J
	10 ps	850 J	850 J	850 J
	100 ps	1500 J	1750 J	1750 J

they are irradiated by the fully compressed pulse and are finely structured optics that require lithographic-like processing to achieve the diffraction properties. It is hypothesized that some of the grating production and cleaning steps have thus far prevented achieving the design energies over the full aperture of the parts. The actual laser performance is pushed as high as can be achieved without damaging the compressor optics; for some pulse durations, the current operating envelope is less than the "full spec" (potential) performance capability. The near-normal deformable mirror after the compressor is also at high risk of laser damage. At a 1-ps pulse duration the laser-damage threshold of these optics is scaled by the square root of the pulse duration, limiting the 1-ps beam to 1 kJ. When Beam 2 is co-propagating with Beam 1, its pulse width at full energy is limited by the *B*-integral accumulated in the beam combiner in the grating compressor chamber. The co-propagated beam can be operated with a shorter pulse width provided that the energy is scaled to maintain constant power. The *B*-integral also reduces the focusability of the beam, leading to a spot radius of 20 μm. A higher *B*-integral can be tolerated for experiments that require a larger spot radius.

The 2014 operational long-pulse performance parameters are given in Table 3.2. For the shorter pulse widths the energy is limited by *B*-integral considerations in the IR portion of the laser. For the longer pulse widths (≥4 ns) the energy is limited by the damage threshold of high-reflector UV mirrors. Ongoing development will lead to the "full spec" (potential) energies quoted.

Table 3.2: Operational Performance parameters of the 351-nm long-pulse beams for flat temporal profiles. Actual performance parameters are maintained on the operations website and can vary from these values. [see https://epops.lle.rochester.edu/docs/EP_performance_envelope.pdf]

Non co-propagating short-pulse (IR) beams		Beam				
On-target energy	Pulse length	1 (current)	2 current	3 (current)	4 (current)	Any beam (full spec)
Square pulse-shape values	100 ps	100 J	100 J	100 J	100 J	100 J
	250 ps	250 J	250 J	250 J	250 J	250 J
	500 ps	500 J	500 J	500 J	500 J	500 J
	750 ps	750 J	750 J	750 J	750 J	750 J
	1 ns	1250 J	1200 J	1250 J	1250 J	1250 J
	2 ns	1950 J	1700 J	2250 J	2200 J	2500 J
	4 ns	2800 J	2400 J	3150 J	3100 J	4100 J
	6 ns	3400 J	2900 J	3850 J	3800 J	5000 J
	10 ns	4400 J	3800 J	5000 J	4900 J	6500 J

3.3 SYSTEM DESCRIPTION

3.3.1 Laser Sources

The Laser Sources Bay (Fig. 3.5) is located between the north and south capacitor bays on the first floor of the facility. Each beam in OMEGA EP has its own dedicated set of laser drivers, referred to as "laser sources." Three different designs are used; one that produces both short and long seed pulses for Beams 1 and 2 (Fig. 3.6), one that produces just long seed pulses for Beams 3 and 4 (Fig. 3.7), and another that is a NIF preamplifier module (PAM) used for beam-smoothing development. The long-pulse sources are similar to OMEGA technology, with a modified regenerative amplifier (regen) to allow for pulse widths up to 10 ns. The short-pulse source employs optical parametric chirped-pulse amplification (OPCPA)[4] to amplify the required bandwidth.

The short-pulse beams (Fig. 3.6) are seeded with a commercial Time Bandwidth Products[5] mode-locked oscillator that produces pulses with a ~200-fs duration and 8-nm bandwidth. These pulses are initially stretched to several picoseconds and amplified by an ultrafast OPA. This initial amplification step optimizes pre-pulse contrast by reducing the nanosecond pedestal that is intrinsic to the latter OPA stages. The pulses are further stretched to ~2.4 ns (FWHM) in an optical system that uses diffraction gratings to impose different delays on different frequency components.[6] The resulting "chirped" beam is spatially shaped before being amplified using an optical parametric amplifier. This OPCPA stage is critical to the performance of the short-pulse beams. Attractive features of OPCPA include a broad gain bandwidth, high gain in a short optical path, and reduced amplified spontaneous emission over conventional laser gain amplification. These features are exploited to preserve the bandwidth of the signal beam and provide a gain of ~10^9.

Optical parametric amplification is a nonlinear optical process wherein energy is down-converted from a (pump) beam of higher frequency into two beams of lower frequency, known as the signal and idler beams. For OMEGA EP, the pump beam is a frequency-doubled, 527-nm-wavelength, Nd:YLF laser. Lithium triborate (LBO) crystals are used as the parametric-amplification media. The signal beam is the input to each OPCPA stage, and the amplified signal beam is the output. The idler (1053 nm, like the signal) is generated in the LBO crystals and separated after each OPCPA stage. The sum of the (chirped) signal and idler frequencies equals the pump frequency for each temporal portion of the pulse. Optical parametric amplification is essentially the reverse of sum-frequency mixing, where two lower frequencies combine to form a higher frequency as in the third-harmonic frequency-conversion crystals, and is described by the same equations.[7] OPCPA is a special case of optical parametric amplification where the signal beam is frequency chirped.

The OPCPA pump laser starts with the same components as the long-pulse beam up to and including the regen and produces a beam that is flat in time. The beam emerging from the regen is spatially shaped using an apodizer to produce a square cross section to match the shape of the beamline optics. It is then amplified to ~2 J/pulse in a high-repetition-rate (5-Hz) power amplifier (CLARA, crystal large-aperture ring amplifier[8]) and converted to 1.4-J, second-harmonic pulses using a frequency-doubling cell. The pump laser, flat in both space and time, is critical to the overall performance of the short-pulse beams. The OPCPA system has reliably produced energies of 400 mJ,

Figure 3.5
Laser Sources Bay.

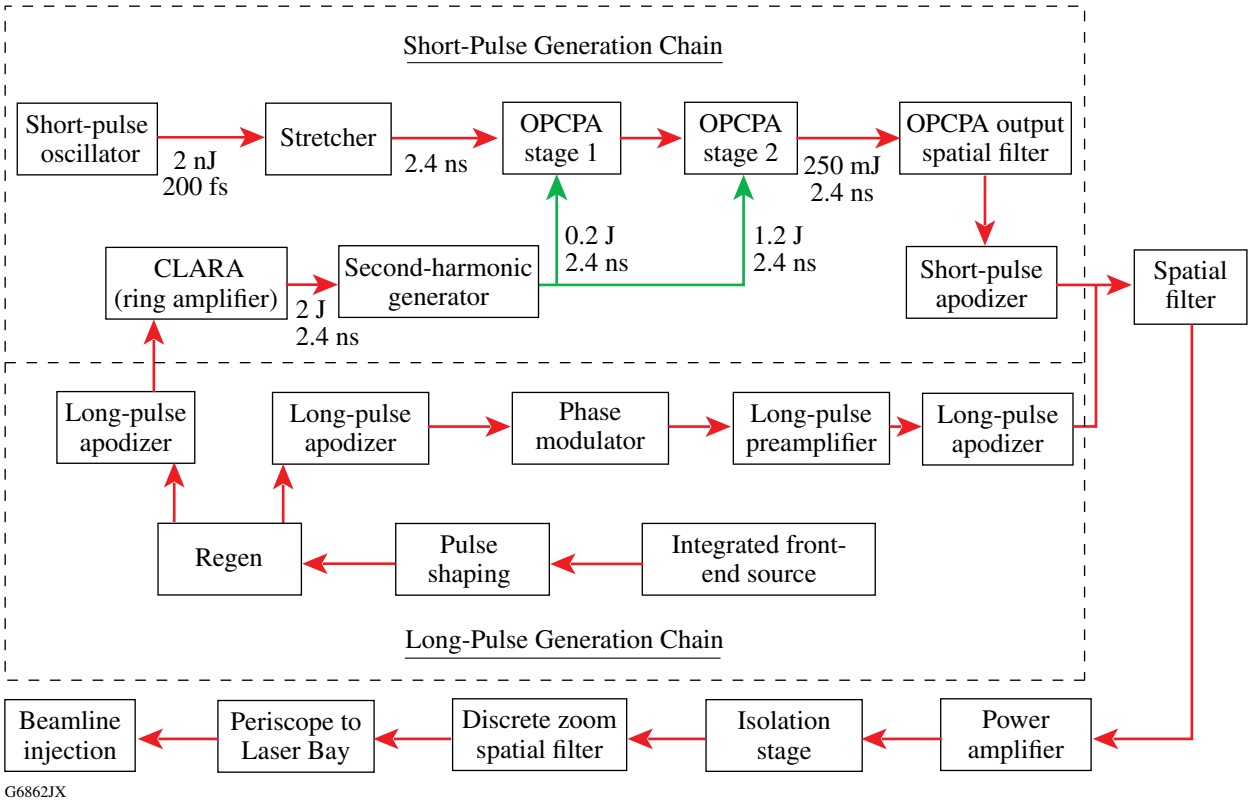

Figure 3.6
Block diagram of the Laser Sources subsystem for Beams 1 and 2. These sources support both short-pulse (1 to 100 ps) and long-pulse (0.1 to 10 ns) operation.

exceeding the required energy of ~250 mJ at 5 Hz in a 1-cm square beam. The beam emerging from the OPCPA stage passes through a second apodizer that adjusts its spatial shape to precompensate for the spatial gain variations in the disk amplifiers. It is then amplified using the same Nd:glass power amplifier that is used in long-pulse mode. This amplifier employs 15-cm disks similar to those used on OMEGA. The output of the OPCPA stage can also be propagated through the main portion of the laser system to establish optical alignment, verify compressor performance, and align the beam transport and focusing systems.

In long-pulse mode, the same systems are used for all beams (Figs. 3.6 and 3.7). The optical signal from the integrated front-end laser source originates from a commercial distributed-feedback fiber laser.[9] The oscillator produces a continuous wave output (at 1053.044 nm) that is sliced and shaped so that the desired on-target temporal profile will be generated after the nonlinear processes of amplification and frequency conversion. The pulse-shaping system uses either aperture-coupled stripline (ACSL)[10] or arbitrary-waveform-generator (AWG)[11] technology, depending on the pulse-length and bandwidth requirements for a given experiment. The temporally shaped pulse is amplified in a regenerative amplifier that produces ~5-mJ laser pulses at 5 Hz. An apodizer shapes the spatial profile of the beam from round to square. A small amount of frequency-modulation bandwidth is imposed to suppress stimulated Brillouin scattering that could otherwise threaten large optics such as the focus lenses. The bandwidth of 0.5 Å (~15 GHz) is applied at a modulation frequency of 3 GHz using a bulk microwave lithium niobate ($LiNbO_3$) modulator. The pulse is passed through a second apodizer to precompensate for spatial gain variations in the disk amplifiers. The pulse is further amplified in a Nd:glass power amplifier and expanded (to 57-mm square) in a spatial filter before injection into the transport spatial filter of the beamlines. The image plane of the long-pulse apodizer is relayed throughout the system.

Although it is not available for general use, the Beam-4 laser can also be produced by a NIF PAM. In FY08, LLNL and LLE transferred an LLNL-assembled NIF PAM for beam-smoothing development. LLE developed a beam-smoothing technique called multi-FM, which is compatible with the NIF. Single-beam laser smoothing is crucial for direct-drive ICF experiments. Laser-driven nonuniformities cause imprinting of short- and long-wavelength mass modulations at the target's ablation surface. These modulations grow during shell acceleration as a result of the Rayleigh–Taylor

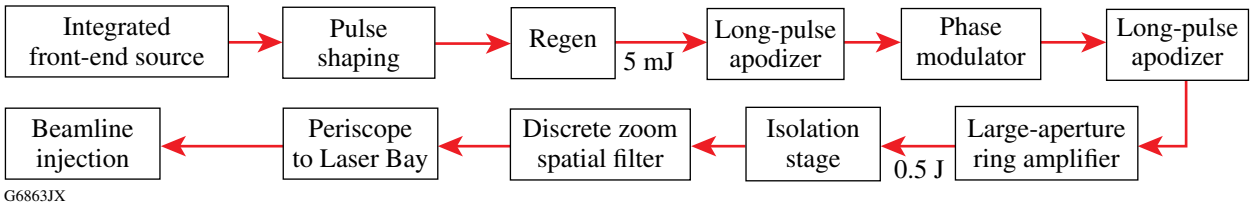

Figure 3.7
Block diagram of the Laser Sources subsystem for Beams 3 and 4. Long pulses of 0.1- to 10-ns duration are provided.

(RT) instability and can lead to shell failure and a significant reduction of target performance. One-dimensional, multi-FM (mFM), smoothing by spectral dispersion (SSD) was developed at LLE to provide the required level of smoothing for the current NIF polar-drive-ignition point design. To demonstrate the efficacy of mFM beam smoothing before implementing this system on the NIF, a prototype mFM seed source was installed and activated on Beam 4 of the OMEGA EP laser and is qualified for limited target experiments (LLE use only). Figure 3.8(a) is a photo of the NIF PAM in the Laser Sources Bay and Fig. 3.8(b) is the rack-mount multi-FM source for the NIF PAM.

Figure 3.8
(a) The NIF PAM was activated on Beam 4 in FY12 to study multi-FM. (b) The multi-FM rack mount hardware provides the input seed with the beam-smoothing features required for on target.

The Laser Sources Bay includes diagnostics that are used for shot preparation and to acquire on-shot laser performance. Measured parameters include energy, temporal pulse shape, spatial profile, spectrum, prepulse contrast, and pulse timing. Energy measurements are accomplished with a centralized 100-channel instrument that is capable of measuring all of the 5-Hz signals, including all of the OPCPA pump-beam energies, and acquiring each of the beam energies on-shot. The energy diagnostic also acquires the beamline output energy from the beamline diagnostic packages. The energy diagnostic is calibrated using absorbing calorimeters at each sample point. Temporal pulse profiles are measured with a multichannel ROSS streak camera. Spatial profiles of the laser beams are captured electronically using 16-bit scientific cameras[12] that image the output plane of each of the laser sources. Beam spectral characteristics are measured with two six-channel, 1/2-meter spectrometers.[13] Prepulse contrast is measured by 7-GHz transient digitizers,[14] and a single-shot cross-correlator after the compressor.[15] An optical time-domain reflectometer[16] uses photodiodes and an oscilloscope to measure stray light that returns to the laser sources after the pulses are delivered to the beamlines. This instrument is used to understand the sources of stray light and their relative magnitude.

3.3.2 Laser Amplifiers and Power Conditioning

The disk amplifiers and their associated power conditioning units are the basic building blocks of the laser, providing the necessary gain and resulting infrared energy. This section describes the booster and main 40-cm disk amplifiers that are located in the Laser Bay. The amplifiers use xenon-flash-lamp–pumped, Brewster-angle, Nd-doped glass disks[17] to provide high and relatively uniform gain across their aperture while avoiding thermal gradients transverse to the laser propagation direction. The basic staging of the 40-cm main and booster amplifiers is similar to that of the NIF.[3] This approach makes it possible for the OMEGA EP Laser System to use a modern multipass design and to benefit from experience gained on the Beamlet[18] and NIF lasers.

The OMEGA EP amplifiers differ from those of the NIF in three ways: (1) OMEGA EP uses a more modular mechanical-design approach than the highly integrated line-replaceable-unit concept[19] used in the NIF, reducing the dependence on expensive robotic handling equipment; (2) the OMEGA EP amplifiers use water-cooled flash lamps[20] to improve the thermal recovery rate; (3) OMEGA-like power conditioning is used to drive the amplifier flash lamps, taking advantage of the commonality with existing OMEGA parts, procurements, and training. A main amplifier consisting of 11 laser disks and a booster amplifier (Fig. 3.9) consisting of 7 disks are used for each of the four beamlines to produce sufficient energy to meet the program's science requirements.

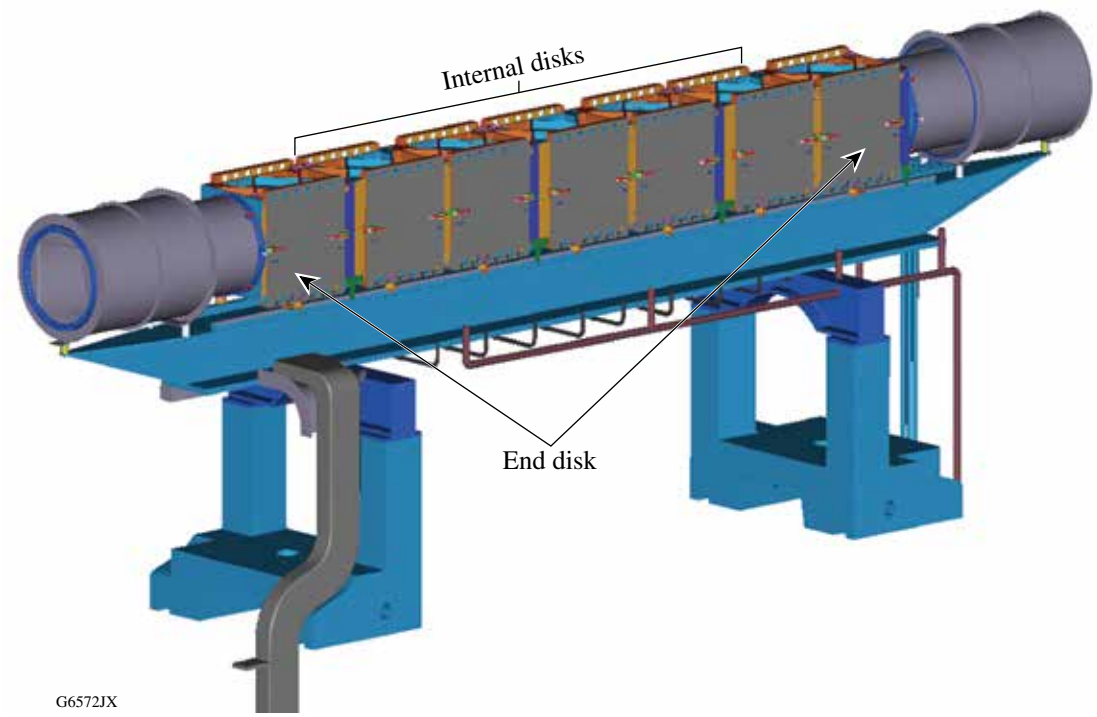

Figure 3.9
7-disk booster amplifier including support structure and beam tubes.

The square beam shape matches the aperture of the amplifiers (Fig. 3.10), maximizing compatibility with the amplifier, adaptive optics, and other components developed for the NIF. The transverse beam cross section is close to being a "flat top" at the end of amplification to maximize the aperture fill factor[21] and the frequency-conversion efficiency, and to minimize the risk of damage caused by excessive amplitude modulation. The beam fits within the 40-cm-sq clear aperture of the amplifiers and the beamline optics, with allowances for alignment tolerances and the lateral beam shift accumulated on each pass through the amplifier caused by the angular multiplexing of the disks.

A measured contour plot of the gain within a typical disk is shown in Fig.3.11(a). Significant variations in the horizontal direction are evident. A nominal gain of ~5%/cm is achieved at the center of the disk, while the edges produce only ~3% to 4%/cm. The problem is magnified because the beam passes through 58 disks in the multipass configuration (two passes through the booster amplifier and four through the main amplifier). Figure 3.11(b) shows the normalized gain along a horizontal lineout after being raised to the 58th power, equivalent to the pulse traversing 58 laser disks.

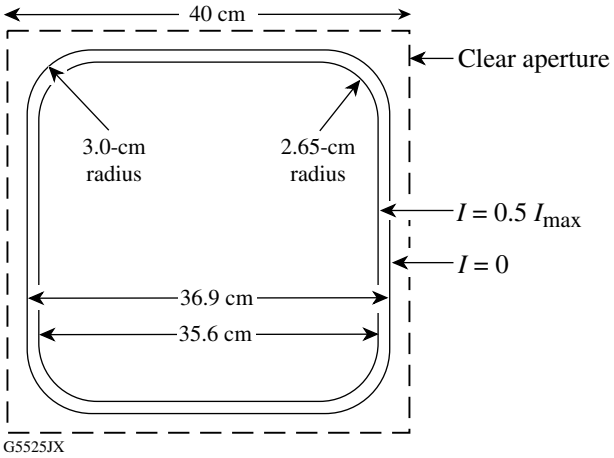

Figure 3.10
40-cm-amplifier beam cross section, showing contours of intensity $I = 0$ and half the maximum intensity I_{max}.

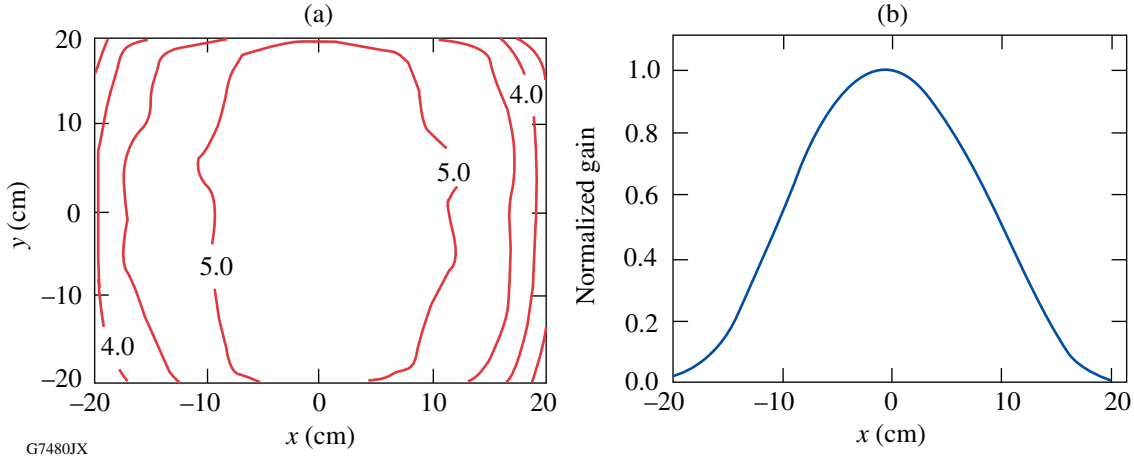

Figure 3.11
(a) Contour plot of gain (in units of %/cm) for an internal disk. (b) Normalized gain along a horizontal slice ($y = 0$) accumulated through 58 disks.

The injected pulse is apodized to compensate for this nonlinear gain profile. Figure 3.12 shows the calculated injection beam shape, with a peak-to-valley ratio of 12.3. The apodizers in Laser Sources, used primarily to make the beam square (following a 40th-order super-Gaussian), filter the energy in the center of the pulse to compensate for the high gain in the center of the amplifier. This ensures that the beams entering the pulse compressor and the frequency conversion crystals have flat spatial profiles.

Most features of the OMEGA EP amplifier modules are similar to those of OMEGA with one notable difference. Each OMEGA disk-amplifier module contains four laser disks, whereas each OMEGA EP amplifier module contains a single disk. This achieves maximum modularity of amplifiers, allowing for an economy of scale for procurement. Each amplifier module consists of three major subassemblies: the amplifier frame assembly, the disk frame assembly, and the pump module, as shown in Fig. 3.13. The pump module system is similar to that of OMEGA and features water-cooled flash lamps. A water-cooled flash-lamp assembly is shown in Fig. 3.14. It consists of a flash lamp, a Pyrex water jacket, and two flash-lamp connector assemblies. The connector assemblies provide the electrical connections to the flash lamp as well as the means for moving cooling water into and out of the assembly.

The power conditioning system provides the electrical energy that energizes the laser amplifiers. A 500-kVA substation supplies power to the power conditioning unit (PCU, Fig. 3.15) at 208 V. This power is converted to high voltage and used to charge a bank of capacitors for subsequent discharge into the flash lamps in the laser amplifiers. The power-conditioning control module in the PCU times this discharge, diagnoses the performance of the equipment during the shot, and provides data to the Power Conditioning Executive software. Each amplifier disk has an associated PCU. The PCU is the building block of the power conditioning system. There are 77 PCU's in the capacitor bays on the first floor of the facility, one for each of the 76 glass amplifier disks and an additional PCU used to support testing. There are seventy-two 40-cm disk amplifiers in the OMEGA EP Laser Bay (eighteen per beam). Laser Sources use four smaller glass amplifiers, each supported by a single PCU.

Each PCU is a self-contained, pulsed-power system that includes (1) a high-voltage power supply to convert incoming ac to high-voltage dc; (2) pulse-forming networks (PFN's) for energy storage and pulse shaping; (3) preionization and lamp check circuits (PILC's); (4) high-energy switching devices to discharge the energy; and (5) an embedded controller with associated control circuits and diagnostics to safely sequence the charge and discharge functions. The pulsed-power circuits are nearly identical to those of OMEGA except that inductance is added to the PILC circuit to generate a pulse with a reduced rise time. Each pulse-forming network powers three amplifier lamps connected in series and is a critically damped circuit made up of a single inductor, capacitor, and resistor. Each PCU is supplied with power from a 2-kW, high-voltage power supply with a 15-kV dc output. The pulse-forming-network capacitors are constructed using metalized polypropylene film technology. This is the industry standard for energy-storage capacitor construction and provides high energy density and excellent reliability compared with the layered-paper and metal-foil construction used in older designs. The switching-style power supplies, used to charge these capacitors, are mounted within each PCU enclosure. The A-size (e.g., Richardson[22] NL-7218H-100) ignitron switches energy for the PILC pulse, and the D-size (Richardson NL8900R) ignitron switches energy into the flash

lamps for the main pulse. These ignitrons are used in the OMEGA Laser System and are proven, robust, and reliable devices. The OMEGA EP power conditioning units contain stand-alone trigger generator modules located at both the PILC and pulse-forming-network ignitrons. These modules enable the power conditioning control module to trigger each of the ignitrons at the appropriate time.

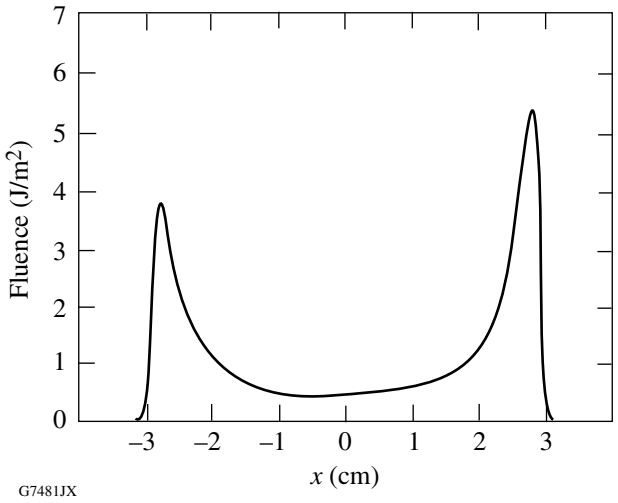

Figure 3.12
Nominal injection beam shape for the four-pass mode of operation.

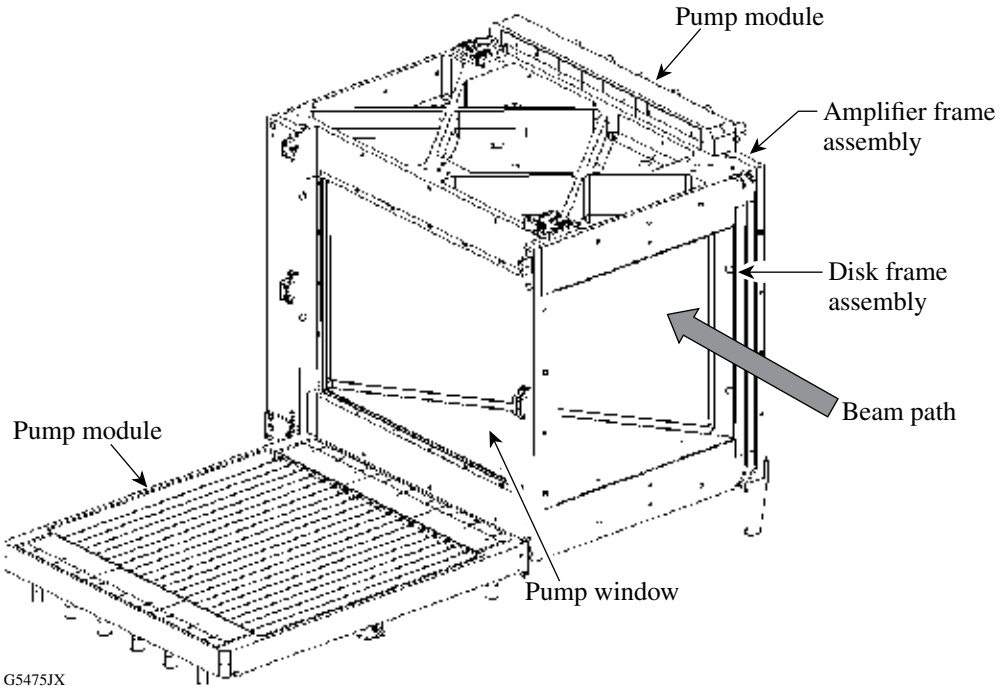

Figure 3.13
Isometric view of an OMEGA EP amplifier module showing the three major subassemblies (amplifier frame assembly, disk frame assembly, and pump module). The path of the laser beam is also shown.

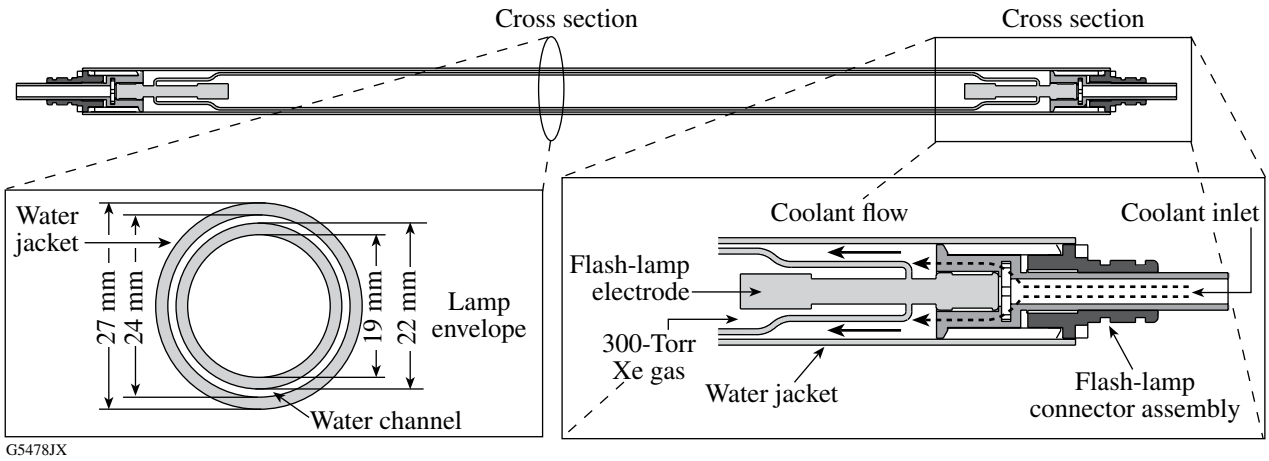

Figure 3.14
Sectional view of a water-cooled flash-lamp assembly.

Figure 3.15
Power conditioning unit. (PFN: pulse-forming network; PILC: preionization and lamp check).

3.3.3 Beamlines

The optical components in the injection and amplification portions of one beamline are almost identical for long- or short-pulse operations. Referring to Figs. 3.3 and 3.6, the input laser beam (up to 0.58 J for 2-ns long pulses, 3.5 J for 10-ns long pulses, and 0.55 J for short pulses) is injected into the transport spatial filter, where it expands to a ~37-cm-sq aperture. The injection lens (Fig. 3.3) is color corrected with a negative-dispersion diffractive optic that precompensates chromatic aberration accumulated from large-aperture beamline lenses. After the expanded beam makes an initial pass through the seven-disk booster amplifier, it is reflected down 1.5 m to the lower beam level by a fold mirror and a Brewster's angle polarizer (POL1) to enter the main laser cavity. This represents a layout change from the NIF to fit the beamlines into a smaller building. The fold mirror is smaller than that of the NIF and has a different coating requirement because of the reduced angle of incidence. The transport spatial filter is shorter than that of the NIF as the image relay distances to the target area are smaller.

The beam must be *p*-polarized relative to the disks in both amplifiers. The amplifier disks are mounted lengthwise on edge to minimize stress, requiring a horizontal orientation of the electric field. The electric field is *s*-polarized relative to the fold mirror and the Brewster's angle polarizer POL1, resulting in maximum reflectance from the polarizer surface.

To permit four passes through the main amplifier, the polarization of the beam must be rotated to prevent the beam from being reflected out of the cavity following the second pass. This is accomplished by the plasma-electrode Pockels cell (PEPC). It is an electro-optic device that rotates the electric-field vector of plane-polarized radiation by 90°. The LLE unit is based on the design developed at LLNL for the NIF. For four-pass operation, the PEPC is initially in its "off" state. After the pulse has passed through the PEPC, the device is switched to its "on" state by applying a high voltage (~20 kV). The returning beam is then rotated to a vertical polarization state, making it *p*-polarized relative to the Brewster's angle polarizer POL1, resulting in high transmission through the polarizer. The beam then reflects from the cavity end mirror and returns through the polarizer and the PEPC. The PEPC rotates the beam's polarization another 90° back to its initial, horizontal orientation. The voltage on the PEPC is then turned off and, following the fourth pass, the beam is switched out of the cavity by POL1 and returns to the upper portion of the beamline.

The deformable mirror[23] at one end of the laser cavity corrects for low-spatial-frequency aberrations (of length scale ≥33 mm) introduced by the amplifier disks. A sample of the output beam, taken immediately after the transport spatial filter, is reflected to a Shack–Hartmann wavefront sensor. The output of the wavefront sensor is used to generate error-correction signals sent to the 39 actuators on the deformable mirror.

The cavity and transport spatial filters use a pair of aspheric lenses housed at the ends of evacuated tube assemblies to spatially filter the light between amplifier passes and to provide relay-plane imaging. The cavity spatial filter relays the image plane of the front-end apodizer to the deformable mirror. North of the transport spatial filter assembly there is a diagnostic beam-splitter mirror that provides a path to beam diagnostics that include shot and alignment sensors. In both the

cavity and transport spatial filters, the beam passes through a different pinhole on each pass through the spatial-filter focal plane. This "angular multiplexing" reduces the likelihood of pinhole closure in the cavity spatial filter. There are four pinholes in each assembly, one for each pass. Angular multiplexing is used in the transport spatial filter to allow the seed beam to be injected into the main beamline.

In short-pulse mode, the Brewster's-angle polarizer POL2 in combination with the PEPC (Fig. 3.3) prevents back-reflected pulses from the target from re-entering the main amplifier. (Back-reflected pulses could extract gain from the amplifiers and damage the injection mirror in the transport spatial filter.) The PEPC is pulsed "on" after the main pulse exits the cavity and prior to the arrival of the back-reflected pulse. Back-reflected light that re-enters the beamline has its polarization rotated by the PEPC and is rejected from the system by POL2 into a beam dump before it can reach the main amplifier disks and deformable mirror. A compensator plate, also at Brewster's angle, is placed next to POL2 to avoid the spatial shift in the beam centerline that results from passage through a single obliquely oriented optic. The polarizer POL2 is not needed in long-pulse mode since any UV light reflected from the target will not reflect off the IR transport mirrors and cannot re-enter the beamline. It is removed from the cavity to avoid damage in this mode of operation.

The components of the beamline are interconnected with nitrogen-filled beam tubes (not shown in Fig. 3.16). This prevents oxygen from degrading the internal silver reflecting surfaces internal to the main and booster amplifiers and maintains the low-relative-humidity working environment required by the polarizer coatings. The tubes and amplifiers are positively pressurized to ~0.1 in. of water. A monitoring system determines the oxygen percentage and relative humidity and can provide an out-of-specification alarm in the Control Room.

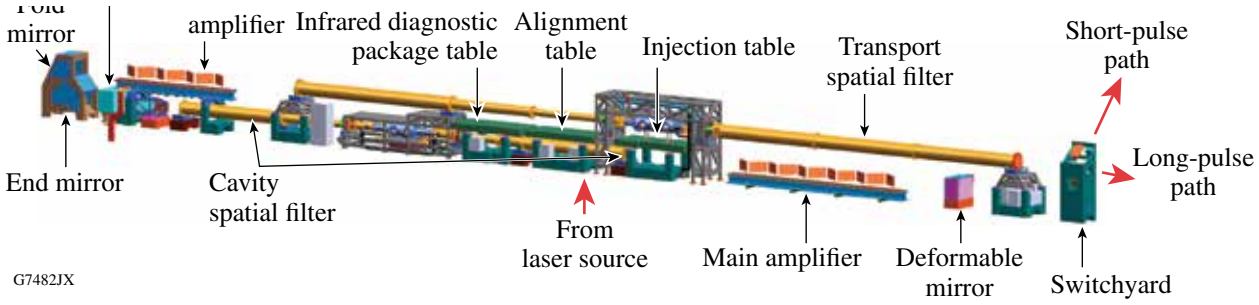

Figure 3.16
Main portion of an OMEGA EP beamline. The laser cavity is formed on the lower level (1.0 m from the floor) between the end mirror and the deformable mirror. The input beam from Laser Sources is injected into the transport spatial filter on the upper level (2.5 m from the floor).

An IR diagnostic package containing a suite of diagnostic instrumentation is dedicated to each of the beamlines (Fig. 3.17). This package provides comprehensive information about system performance in preparation for and during a target shot. During a shot, measurements are made of the beam energy, the near-field and far-field spot profiles, and the full-aperture beam wavefront. A spectrometer and a streak camera are used to measure the temporal pulse shape. Prior to taking a shot, alignment diagnostics are used to point and center the beam from the source injection point to the beam emerging from the end of the transport spatial filter.

The source beam for the IR diagnostic package comes from the first-surface reflection of the IR diagnostic beam splitter—a flat, wedged plate oriented at 0.10° relative to the beam normal and located at the output end of the transport spatial filter (Fig. 3.17). Approximately 0.2% of the incident light is reflected from the front surface of this plate and down-collimated by the transport-spatial-filter output lens and a lens on the pinhole table within the transport-spatial-filter vacuum vessel.

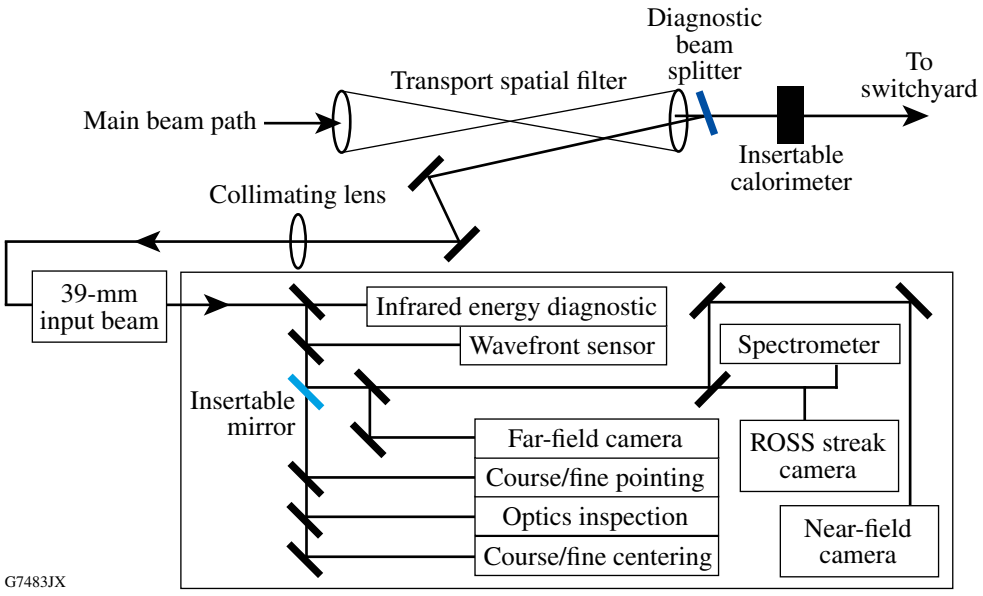

Figure 3.17
Schematic layout of the infrared diagnostic package (placed on a 5-ft × 12-ft optical table near the transport-spatial-filter injection point), identifying the beam paths to the nine individual instruments. The beam is sampled after emerging from the transport spatial filter. The insertable mirror is removed during alignment procedures prior to a laser shot.

3.3.4 Pulse Compression, IR Short-Pulse Transport, and Diagnostics

The pulse-compression grating systems are located in the grating compressor chamber—a large rectangular vacuum chamber in the northwest corner of the Laser Bay (Fig. 3.18). An equipment entry door on the south end facilitates insertion of large pieces of equipment, while two smaller entry doors located on the north and south ends provide personnel access.

Referring to Figs. 3.19 and 3.20, the grating compressor chamber houses two independent pulse compressors, deformable mirrors, compressor alignment mirrors, transport mirrors, a beam

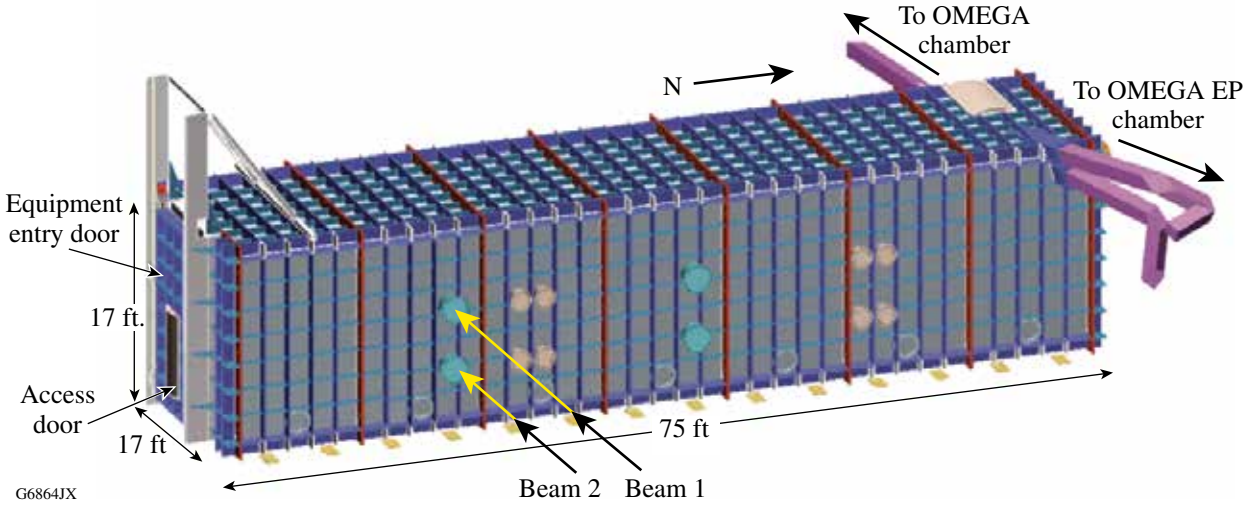

Figure 3.18
Grating compressor chamber (GCC), showing the main equipment access door to the south and the beam exit ports to the north.

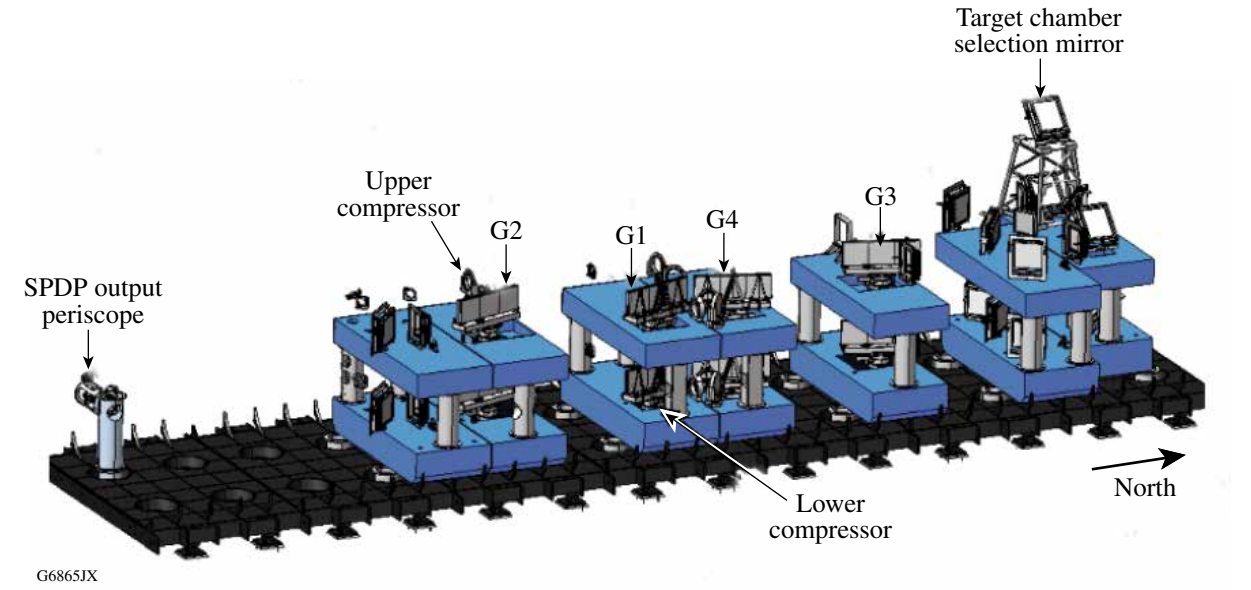

Figure 3.19
Internal components of the GCC, including the tiled grating assemblies (G1 to G4) and the target-chamber selection mirror. The upper and lower compressors, for Beams 1 and 2, respectively, are aligned atop one another. Diagnostic beams exit the GCC via the short-pulse-diagnostic-package (SPDP) output periscope.

combiner, and transport optics to the short-pulse diagnostic package table. Each pulse compressor comprises four tiled grating assemblies (G1 to G4), each of which comprises three tiled gratings. A pair of interferometers align the tiles of each tiled grating assembly. Insertable full-aperture calorimeters are inserted to measure the energy of the high-intensity pulses and calibrate on-shot energy diagnostics. There are 14 optical tables within the grating compressor chamber.

The optical path of the upper compressor is shown in Fig. 3.20. Beam 1 from the switchyard enters via a vacuum window located on the east side of the grating compressor chamber and is directed toward the first grating assembly, G1, at an incidence angle of 72.5º. The diffracted beam (at 61.5º) encounters the second grating assembly (G2) at 61.5º and emerges at 72.5º. After similar paths through G3 and G4, the pulse has been temporally compressed by up to 300 ps/nm. Emerging from G4, the pulse reflects off the compressor deformable mirror, which corrects for aberrations in the compressor optics and the short-pulse transport and focusing optics. The diagnostic mirror directs 0.5% to 1% of the energy to the short-pulse diagnostic table. The remainder of the pulse reflects off the surface of the beam-combiner mirror to the target-chamber selection mirror. The design of the lower compressor is virtually identical; however, after the diagnostic mirror, the pulse may follow two paths. It may transmit through the beam combiner, where it becomes co-aligned with the pulse from the upper compressor and is directed either to the OMEGA target chamber or to the "backlighter" port of the OMEGA EP target chamber. Alternatively, it may be routed independently to the "sidelighter" port of the OMEGA EP target chamber.

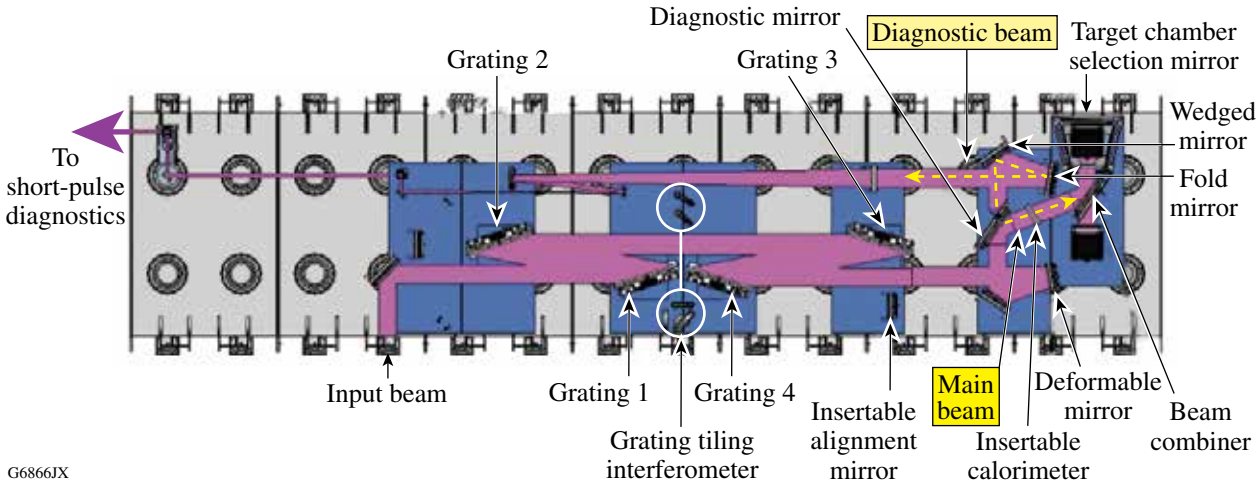

Figure 3.20
Optical path of the upper compressor. The diagnostic mirror provides a 1% pickoff for the short-pulse diagnostic beam, shown exiting the chamber to the left. The optical configuration of the lower compressor is almost identical. The circles are the internal structure mounting points. (Note: The final design differs from this figure in some minor details.)

A photograph of a grating assembly is shown in Fig. 3.21. The width of the assembly accommodates the beam footprint at 72.5º. Three smaller gratings (47 cm wide by 43 cm high), rather than one large grating, were designed to facilitate their manufacture. The grooves of the gratings are aligned with the vertical and have a pitch of 1740 grooves/mm. The outer tiles are precision aligned to the center tile to control tip, tilt, rotation, piston, and shift using an interferometer incorporated into the compressor, minimizing errors in the combined wavefront. The tiles rest upon a precision six-axis stage for compressor alignment.

G6867JX

Figure 3.21
Grating assembly, comprising three tiled gratings on a tile support beam placed on a six-axis base used for compressor alignment. Each of the outer grating tiles has a precision control system used to align the beam wavefront to that of the center tile.

The components on the two optical tables to the north of the compression gratings comprise the short-pulse switchyard. Configuration flexibility allows for the short-pulse beams to be delivered to the OMEGA or OMEGA EP target chambers. The different configurations are obtained by positioning the upper mirrors of two periscopes to the desired locations (Fig. 3.22).

The instruments in the short-pulse diagnostic package (Fig. 3.23) diagnose the properties of the beams before they are co-aligned. They measure the beam quality, energy, alignment, spectrum, optical component damage, output wavefront, pulse width, and pulse contrast. For the upper beam, the transmitted light through the diagnostic mirror in the grating compressor chamber is directed to a near-normal-incidence optic with a slight wedge. The first surface of the wedge is uncoated, providing a 4% reflection, while the rear surface of the wedge is highly reflective. The small pointing difference between the beams reflecting off the front and rear surfaces of the wedge allows an operator to select either a low- or a high-transmission path. This flexibility enables greater attenuation for the highest-intensity (~1-ps) short-pulse beams, providing a low-energy diagnostic beam and minimizing the *B*-integral for on-shot measurements. The lower compressor generally operates at 10 to 100 ps

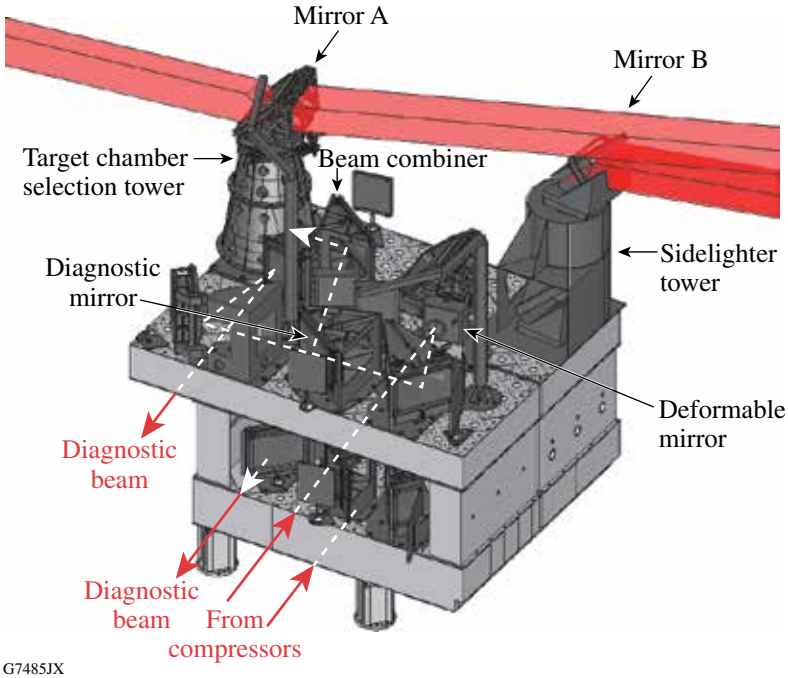

Figure 3.22
Short-pulse switchyard. Co-propagated or individual beams can be diverted to either chamber by the two-position mirror (A). The beam from the lower compressor is periscoped up to the upper table, where it is directed by the two-position mirror (B) either through the beam combiner or to the sidelighter tower.

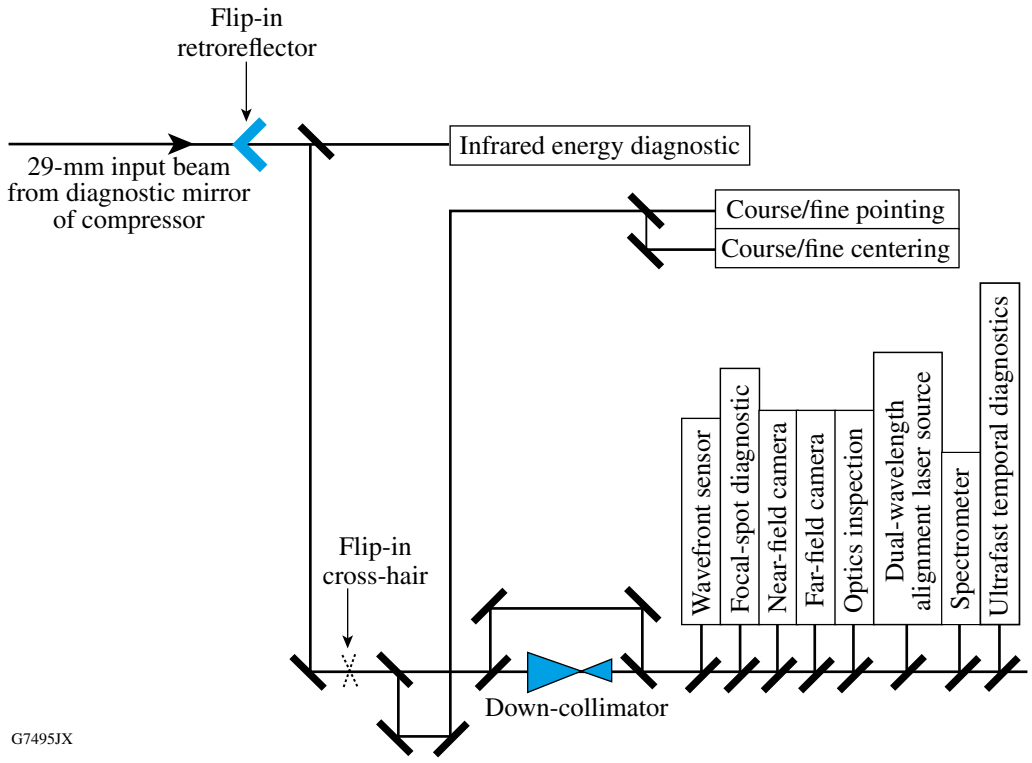

Figure 3.23
Layout of the short-pulse diagnostic package. There is one of these systems for each of the two compressed beams.

and does not need an attenuation wedge. A single 45º fold mirror in the lower compressor beam replaces the wedge and fold mirror pair. In both compressors the diagnostic beam is downcollimated by a pair of lenses.

The diagnostic package includes a dual-wavelength IR alignment laser (1053 nm and 1047 nm) that can illuminate the short-pulse transport paths to the target and the Fizeau interferometers in the grating compressor chamber. This laser allows for alignment and setup of the pulse compressors to be conducted independently of the main beamline. Two wavelengths are used in the alignment procedure to ensure that the grating assemblies are aligned for broadband compression. The short-pulse diagnostic package sends this laser beam into the compressor counter-propagating to the pulsed beams. Insertable alignment mirrors in the compressor allow for fine positioning of each of the grating degrees of freedom. One of these alignment mirrors directs the dual-wavelength laser back to the target chamber along the short-pulse transport path. The diagnostics and laser source are located on a 5-ft × 32-ft optical table adjacent to the compressor vessel. The instruments in the short-pulse diagnostics package (Fig. 3.23) are nearly the same as those on the infrared diagnostic package at the output of the transport spatial filter. Alignment sensors, near- and far-field cameras, energy sensors, wavefront sensors, and inspection systems are also used. Unique to this area are the focal-spot diagnostic and the ultrafast temporal diagnostic package. The focal-spot diagnostic uses pre- and on-shot wavefront sensors and near-field spatial-profile instrumentation to characterize the spatial irradiance pattern on target. A far-field camera with two fields of view is used pre-shot (in narrow field) to confirm grating tiling alignment and on-shot (in wide field) to characterize any noise passing through the pinholes. The temporal instruments consist of a fast streak camera and an autocorrelator used in combination to measure the pulse duration and shape. The flip-in retroreflector in Fig. 3.23 is used for various alignment procedures.

After the laser pulses are compressed in the grating compressor chamber, they are transported to target by reflections off mirrors within a vacuum environment. Each of the three available beam paths includes at least two steering mirrors and one focusing mirror, an *f*/1.8 off-axis parabola with a 1-m focal length. The path from the grating compressor chamber to the OMEGA target chamber is shown in Fig. 3.24 and the path to the OMEGA EP target chamber in Fig. 3.25. The vacuum vessels have gate valves at either end to isolate the tube and mirror enclosures to direct the beam to the focusing parabola.

The off-axis parabola requires precise alignment to the optical axis of the system, accomplished using the vacuum-compatible parabola alignment diagnostic (shown in Fig. 3.26). This diagnostic is placed in a ten-inch manipulator. It includes a linearly polarized, fiber-coupled laser apodized to the OMEGA EP spatial profile with its polarization rotated by a waveplate to match the incoming beam. This alignment beam can be counter-propagated through any of the transport paths and directed by an insertable compressor alignment mirror into the short-pulse diagnostic package. The alignment diagnostic also senses the wavefront of the short-pulse diagnostic package beam using a lenslet array and a CCD camera, and the beam pointing using a lens and CCD camera. Wedges in the parabola alignment diagnostic compensate for the keystone distortion of the off-axis parabola. The parabola alignment diagnostic is positioned to the desired focus of the short-pulse beam and a target-chamber–referenced autocollimator, bringing the beam onto the target along the proper axis.

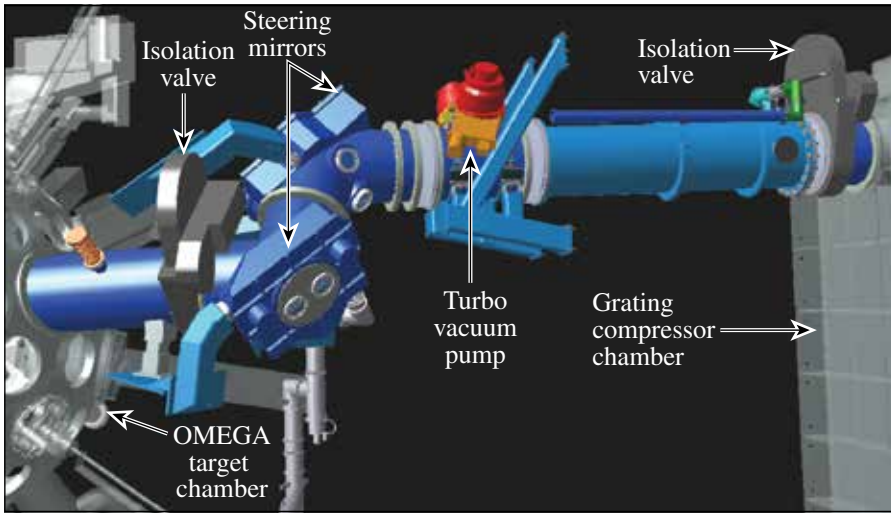

Figure 3.24
Short-pulse path from the grating compressor chamber to the OMEGA target chamber.

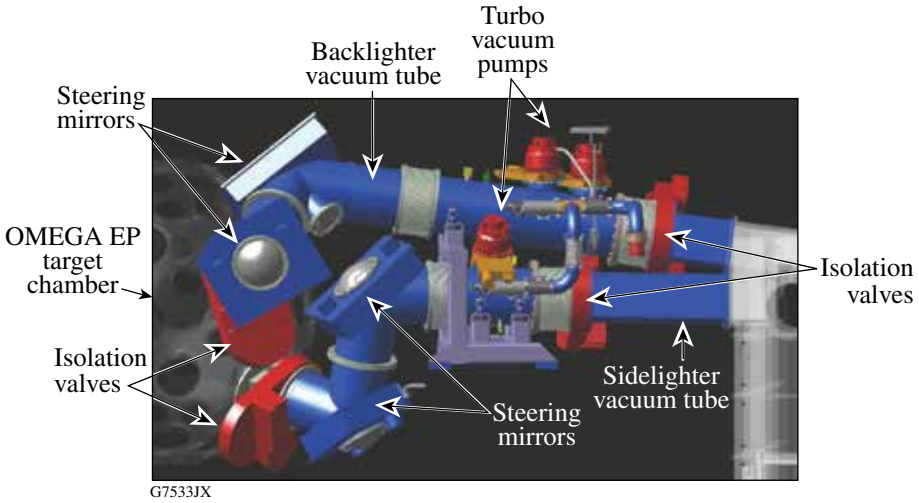

Figure 3.25
Short-pulse path from the grating compressor chamber to the OMEGA EP target chamber.

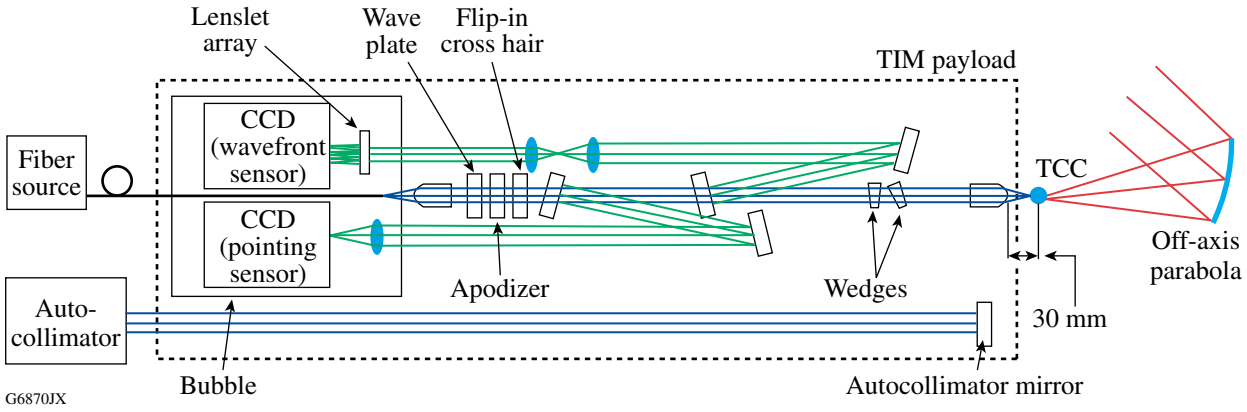

Figure 3.26
Parabola alignment diagnostic (PAD), a self-contained TIM-based diagnostic, portable between target chambers. A Shack–Hartmann sensor uses a lenslet array to measure the wavefront reflected off the off-axis parabola, the autocollimator monitors angular displacement of the PAD optics, and a pointing diagnostic determines the location of target chamber center (TCC).

3.3.5 Frequency Conversion, UV Long-Pulse Transport, and Diagnostics

For experiments requiring long-pulse (1 to 10 ns) beams, the 1053-nm beams are frequency tripled to 351 nm using potassium-dihydrogen-phosphate (KDP) and deuterated-potassium-dihydrogen-phosphate (KD*P) frequency-conversion crystals (FCC's) and transported to the OMEGA EP target chamber (Fig. 3.4). They cannot be directed to the OMEGA target chamber. Each beam is focused onto the target using an *f*/6.5 aspheric lens of 3.4-m focal length followed by a vacuum window and a thin debris shield. A phase plate can be inserted before the lens to smooth and tailor the target-plane profile. There are phase plates for all beams that produce 750-μm-diam circular spots, and two additional plates that produce 1.1-mm and 2.0-mm spots. The beams are directed to ports at a 23° angle of incidence with respect to a common central axis that is typically aligned with the target normal.

The frequency-conversion system is based on the type-I/type-II angle-detuning configuration originated at LLE[24] and implemented on the NIF.[25,26] The NIF design has been adopted because it is optimal for OMEGA EP. Two 40 × 40-cm crystals are used: an 11-mm-thick, type-I KDP doubler that converts approximately 67% of the IR to its second harmonic followed by a 9-mm-thick KD*P tripler to mix this second harmonic with unconverted IR to form the third harmonic. Compared with the type-II/type-II polarization-mismatch scheme[24] used on OMEGA, this configuration has the advantage that a polarizer is not needed before the crystals but the disadvantage of a tighter alignment requirement on the doubler for the highest operating intensities. The choice of configuration is forced because transmission polarizers at the IR fluences of the NIF or OMEGA EP are unavailable. An additional consideration is that the type-I cut is more favorable for doubling a square beam due to boule-size considerations.[25]

The frequency-conversion performance is diagnosed with a 4% diagnostic pickoff located after the FCC's in an arrangement similar to that on OMEGA (Fig. 3.27). The pickoff diagnostics include alignment sensors for co-aligning a UV alignment source to the IR alignment source. Each of the four beamlines has its own UV diagnostic and alignment table, located near the target chamber on the target-area structure (Fig. 3.28). The UV alignment source is located on its own table on the Laser Bay floor in front of the target area structure, and its output beam is introduced just before the FCC's with a periscope mirror assembly similar to that on OMEGA (Fig. 3.4). The UV alignment beam is sequentially propagated through each of the four pulsed beam paths. The placement of the FCC's before the target chamber (rather than on the target chamber as in the NIF) permits more convenient beam diagnostics and allows for the rejection of unconverted light by the transport mirrors.

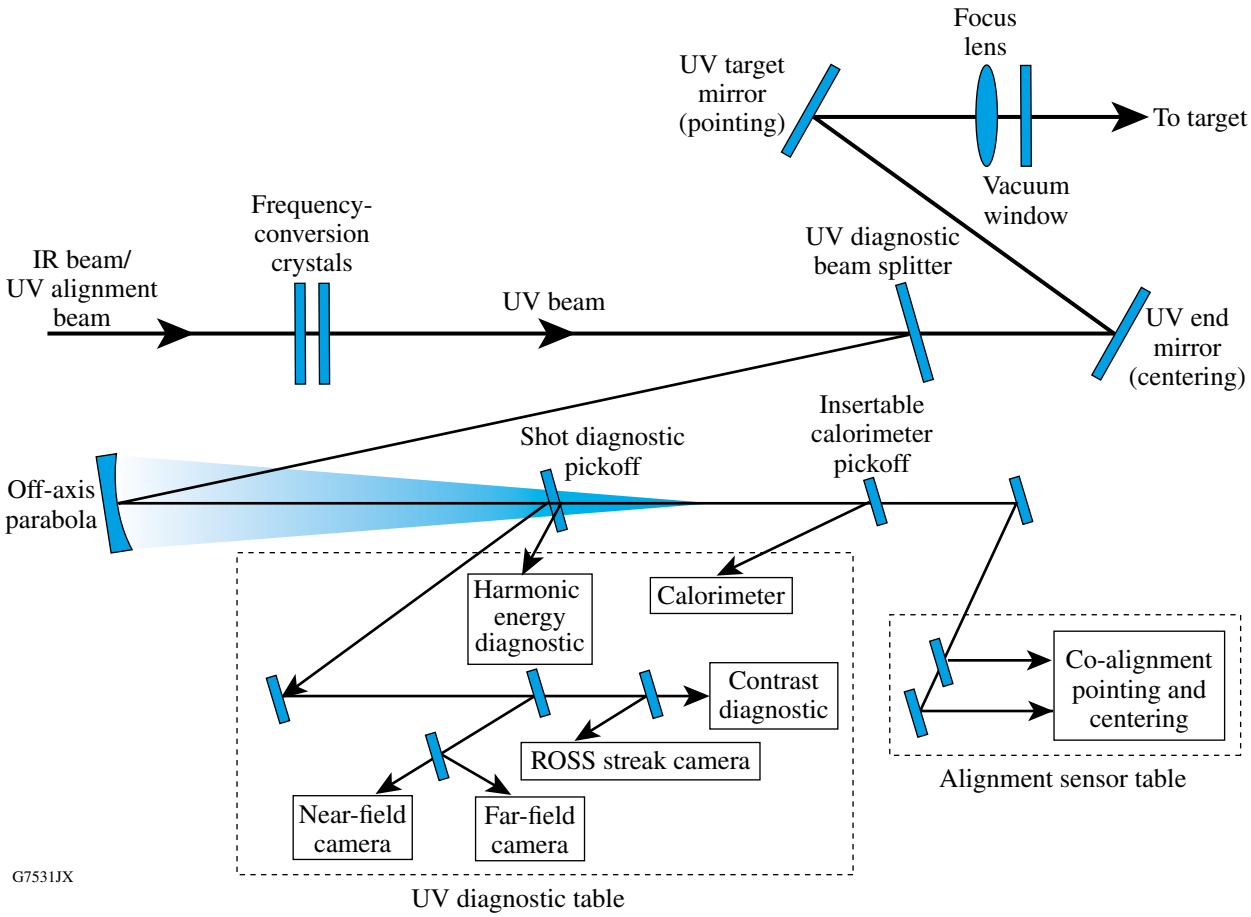

Figure 3.27
Layout of the UV diagnostic table and alignment sensor table.

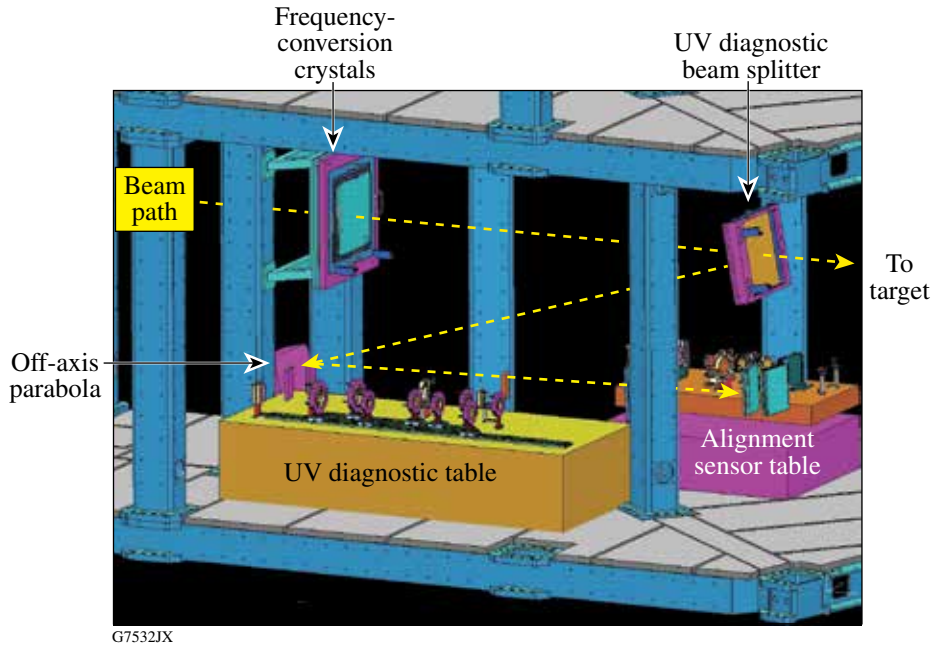

Figure 3.28
Location of the UV diagnostic table and alignment sensor table on the target-area structure.

The UV diagnostic packages provide comprehensive information about the system performance, both in preparation for and during a target shot. Measurements are made of the beam energies at all three harmonics, the near-field (IR and UV) and far-field spot profiles, and the contrast. The IR beam energies before the FCC's are measured in the IR diagnostic package (Fig. 3.17).

Co-alignment of the IR and UV alignment beams is achieved by steering the periscope mirrors to point the UV alignment beam to the pointing and centering alignment sensors on the UV diagnostic table. These sensors use achromatic optics so that they can function at both wavelengths. The portion of the UV alignment beam that passes through the UV diagnostic beam splitter is then steered to the target by moving the transport mirrors (Fig. 3.27). The beam is confirmed to be aligned by retroreflection back to sensors adjacent to the laser source. This method of UV system alignment is the same as used on OMEGA. A minor difference is that the UV beam is injected prior to the FCC's on OMEGA EP.

3.3.6 Target Chamber and Experimental Systems

The OMEGA EP target chamber is similar in design to the OMEGA target chamber and has the same 3.3-m diameter. The chamber is located within the target area structure (Fig. 3.29) located at the north end of the Laser Bay. A diagram of the ports as viewed from the Laser Bay is shown in Fig. 3.30.

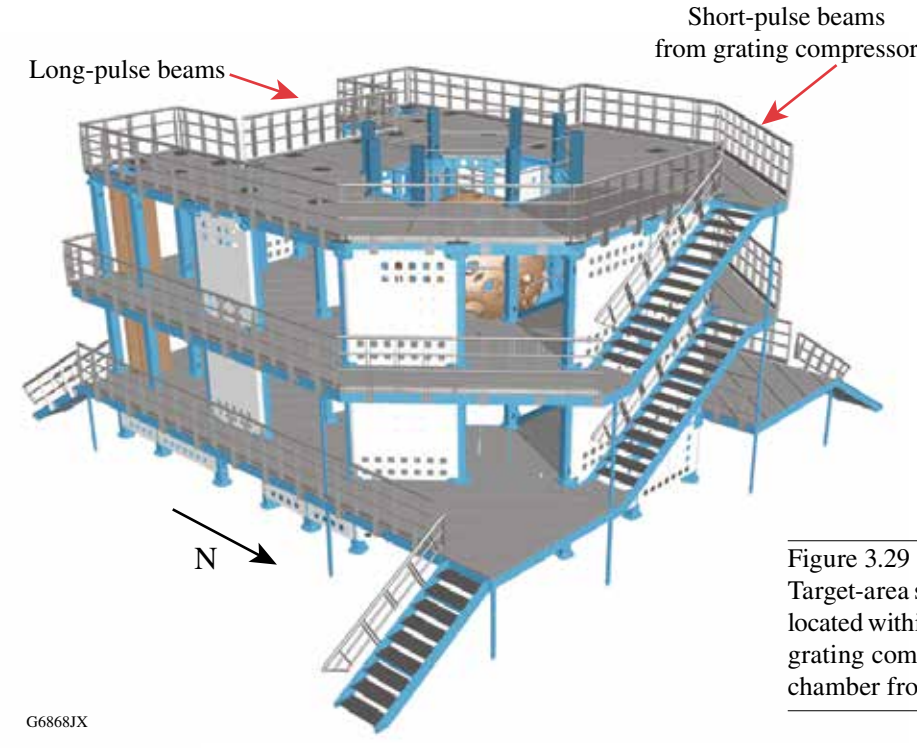

Figure 3.29
Target-area structure with the target chamber located within. Beam-transport tubes from the grating compressor chamber enter the target chamber from the west (not shown).

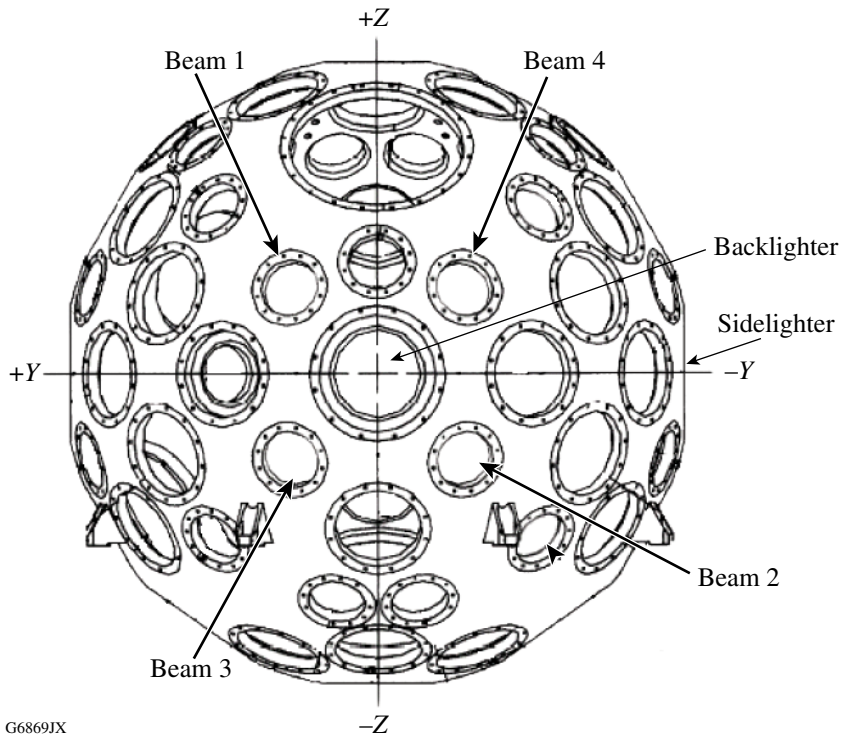

Figure 3.30
South elevation view of ports on the OMEGA EP target chamber. The long-pulse UV beams enter through ports 23º from the central port. The backlighter off-axis parabola resides in that central port ("–X"), and the sidelighter off-axis parabola resides in the "–Y" equatorial location.

The target chamber design takes advantage of the substantial infrastructure developed for the OMEGA Laser System and allows for the full compatibility of existing diagnostic instrumentation. The target chamber has five ten-inch-manipulator (TIM) diagnostic shuttles, two target-positioning systems, a target viewing system, and other support items based on their OMEGA equivalents. The top and bottom ports are reserved for the addition of a planar cryogenic target system. The target chamber has two TIM-like off-axis-parabola inserter/manipulators. Beam transport tubes from the grating compressor chamber enter the target chamber from the west. The short-pulse beams propagate to their respective off-axis parabolas that focus them along orthogonal paths, with the parabolas placed in the "backlighting" and "sidelighting" ports. The target-area structure supports the IR transport mirrors, the periscope mirror assembly, the frequency-conversion crystals, the UV diagnostic beam splitters, the UV diagnostic tables, the alignment sensor tables, and the UV end and target mirrors.

The diagnostic suite has both fixed and flexible diagnostic platforms (see Chap. 5). Fixed diagnostics include plasma calorimeters, x-ray pinhole cameras, Kirkpatrick–Baez microscopes, and x-ray streak cameras. Flexible accommodations for experimental diagnostics are provided by the TIM's. Each TIM provides mechanical, vacuum, and electrical/ control support and positioning for any compatible instrument that must be positioned near the center of the target chamber. The Experimental Systems are described in detail in Chap. 4.

3.4 CONTROL SYSTEMS

3.4.1 Overview

The control system for OMEGA EP is nearly identical to that used on OMEGA. Applications are grouped by functional area and run under a software executive that continuously monitors software status. The control system architecture (Fig. 3.31) shows the hierarchical structure of executive software and the connectivity path that functions when the OMEGA EP beams are used in the OMEGA target chamber. For shots on OMEGA that require OMEGA EP, the OMEGA EP system is treated as a single additional control connection. Operations staffing places control of the executive software under the direction of a single individual in a centrally located control room. The control room for OMEGA EP (Fig. 3.32) has four primary workstations with fixed functions and three flexible workstations for the scientific oversight of operations, maintenance operations, and (on an as-needed basis) concurrent alignment, diagnostic setup, or other testing needs.

The primary control systems consist of beam motion controls for moving devices, video for alignment, and the hardware timing system. These applications and hardware are replicas of the systems in use on OMEGA. Specialized control systems, unique to OMEGA EP, are in place for managing advanced technologies such as the deformable mirrors, the plasma-electrode Pockels cells, Shack–Hartmann wavefront sensors, grating alignment, and a higher precision timing system. The control system architecture has been modified to reflect OMEGA EP as a subordinate system to OMEGA when in the "joint" shot mode. When not shooting jointly, the two laser systems are mostly independent; for some shot configurations the hazards can require closed access on the opposite facility.

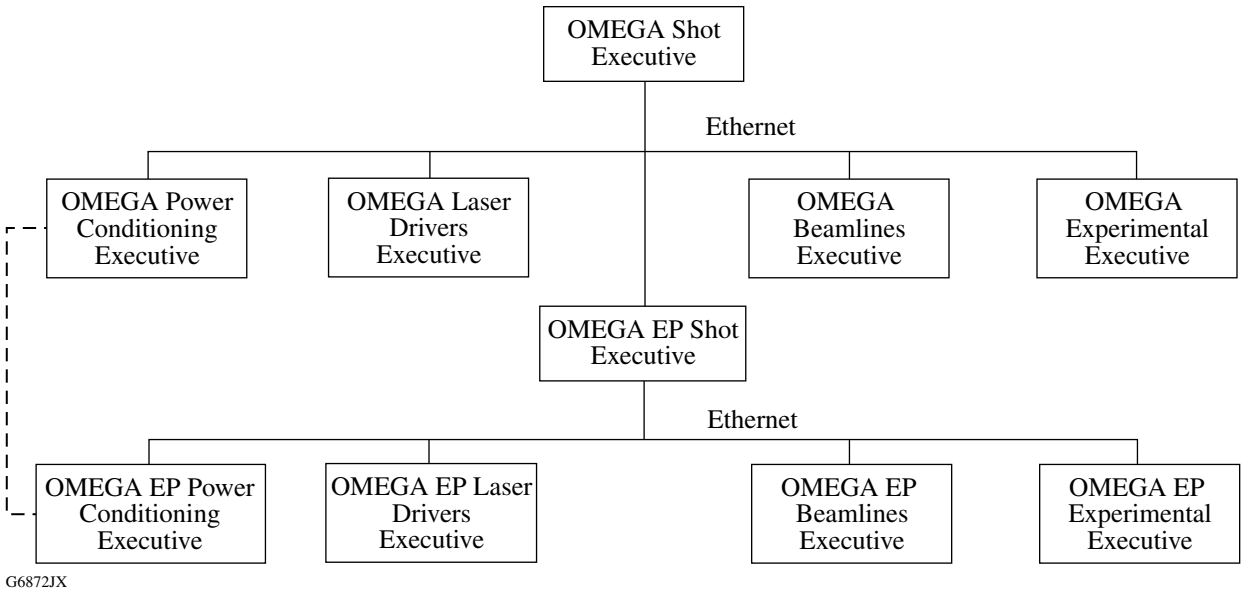

Figure 3.31
Top-level architecture of the laser control system, indicating OMEGA as the senior system when used in joint shot operations. The lines connecting the executives represent the LLE Ethernet and the software hierarchy. Power conditioning executives share information during shot set-up to coordinate charge sequences.

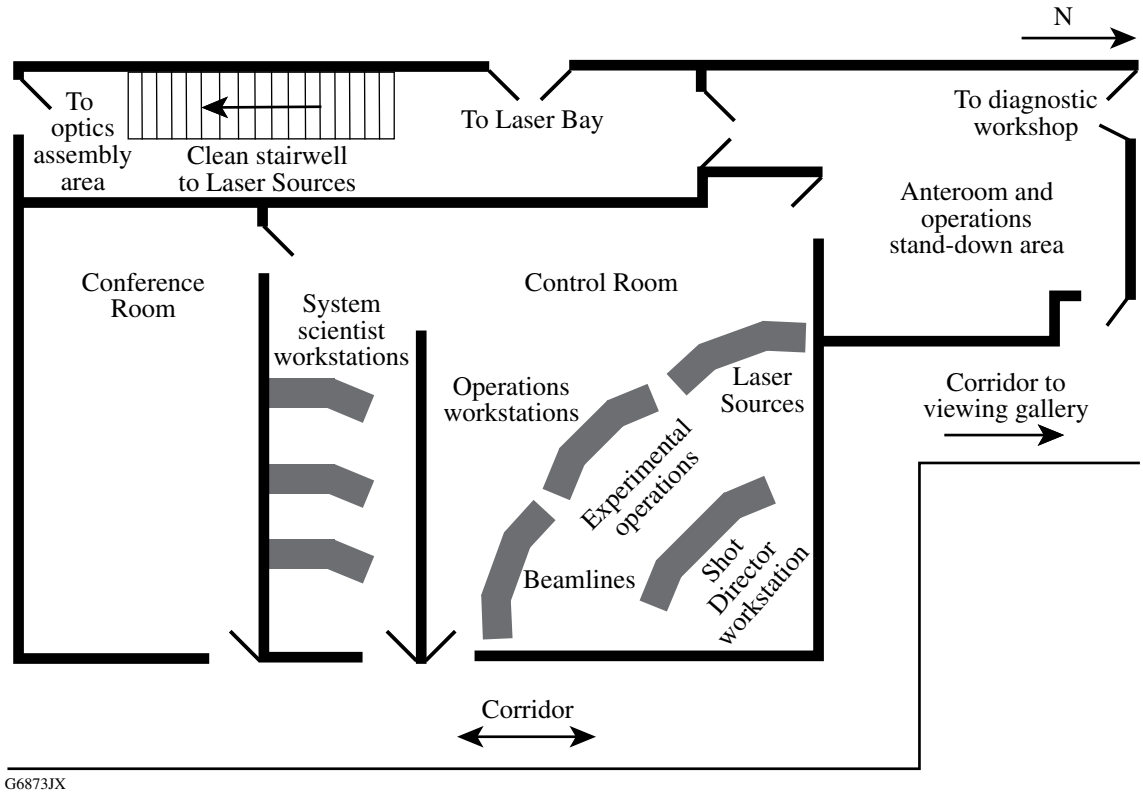

Figure 3.32
Layout of the OMEGA EP Control Room, anteroom, and conference area. Workspace is provided for the system scientists and principal investigators.

As on OMEGA, the laser control system facilitates the operational activities that maintain the system, prepare it for a shot, execute the shot, and record the shot results. A network communication system coordinates actions requiring synchronization to within ~1 sec. The timing required to execute and diagnose a shot is provided by the hardware timing system. A "handoff" between the two levels of timing control takes place 20 s before a shot is triggered. As on OMEGA, the operations system makes use of the concept of a "shot cycle," consisting of a sequence of "system states" and "shot types." The system states partition the activities into known situations for communications and coordination. The shot types identify the configurations in which the high-energy, pulsed beams are propagated and the degree of system-wide coordination that is required. The Shot Executive controls the transitions from one state to the next and ensures that the required sub-executives are performing satisfactorily.

The Shot Director in the OMEGA EP Control Room operates the Shot Executive and the OMEGA EP Power Conditioning Executive. The Power Conditioning Executive is a software program that controls the laser amplifier power conditioning units through a shot sequence. It is similar to the OMEGA Power Conditioning Executive in appearance and function. For shots into the OMEGA target chamber, the OMEGA Power Conditioning Executive is superior, and the charge sequence starts at the command of the OMEGA Shot Director.

3.4.2 Timing Systems

Figure 3.33 shows the timing and shot control configuration for the two laser systems. The reference frequency generator (RFG) is common to both systems, and the 38-MHz sine wave from the RFG is distributed to both facilities. This signal is used in the Laser Sources subsystems and as the precision clock source in each of the timing crates in both facilities. It is used by the master timing generator (MTG) to produce a digital trigger that repeats at a 0.1-Hz rate. This signal is distributed to all of the timing crates along with the signal from the RFG. The 5-Hz signal and other timing signals produced by the timing crates are based on the 38-MHz clock and are synchronized to the MTG 0.1-Hz signal. The Power Conditioning Executive causes the MTG to produce T–10 and T–0 shot triggers synchronized to the 0.1-Hz signals at the correct times in the shot cycle.

The 38-MHz RF and the other (digital) signals used by the Hardware Timing System are distributed throughout the OMEGA and OMEGA EP facilities. The rate regenerator module in each timing crate accepts the RF signal, the 0.1-Hz rate, and the T–10 and T–0 digital signals from the MTG and provides them to quad-channel delay modules. Each delay module has four independent channels that can each be set to implement a precision delay and provide a trigger at the desired amplitude, duration, and rate to one of the seven output signals.

Timing of the laser shot is accomplished by the synchronization of the front-end sources in OMEGA and OMEGA EP using high-bandwidth, ultrafast ROSS streak cameras.

Using streak cameras in the IR at the front end and in the UV at the output, the on-target beams can be timed to 20 ps as on OMEGA. A fiducial pulse can be simultaneously streaked with the main beam. The fiducial is used to determine the relative timing of each of the beamlines with

respect to each other and to the OMEGA beamlines. The fiducial also provides a set of evenly spaced pulses that are used to check the accuracy of the streak-camera time base.

The Precision Optical Timing and Triggering System (POTTS) is an all-fiber-optic signal delivery system that provides precision trigger signals (to 10-ps rms) to the pulse-shaping systems.

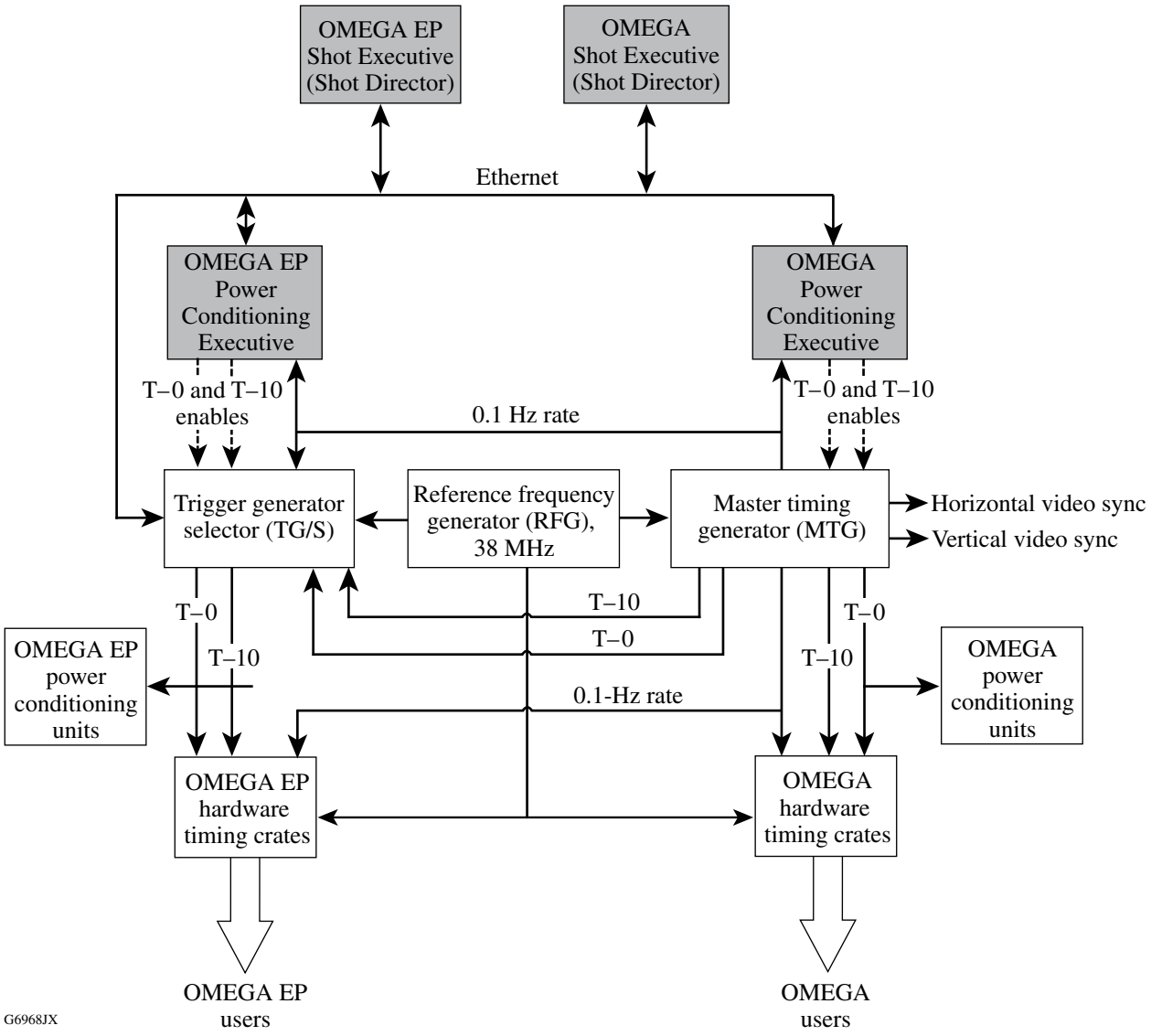

Figure 3.33
Block diagram of the timing control system for joint shot operations. The reference frequency generator is common to both OMEGA and OMEGA EP sytems. The shot triggers used in the OMEGA EP system are distributed by a trigger generator/selector unit that has separate modes for independent and joint operations. In the independent mode, the trigger generator/selector passes synchronized T–l0 and T–0 shot triggers for OMEGA EP only. In the joint mode, the signals generated by the master timing generator are used in both systems.

3.4.3 Alignment Systems

Laser alignment begins as the beam emerges from the fiber optics in the Laser Sources area and continues to the target. The OMEGA EP alignment system partitions this activity into four distinct sections: (1) laser sources; (2) beamline to transport-spatial-filter output; (3) compressor and short-pulse transport; and (4) frequency-conversion crystals to target. The alignment systems rely on sensor systems and control points that are similar to the OMEGA system, largely centering the beam on a single cross hair and then aligning the crosshair to other crosshairs while maintaining the pointing of the laser beam with far-field detectors.

Pointing and centering cameras are used at each of three stages in the laser sources, along with computer-actuated mirrors that can be used to compensate for small amounts of alignment drift. Throughout the system, including the laser sources, large alignment errors at any stage require corrective maintenance.

Each of the main beams has an alignment laser at 1053 nm located on the infrared alignment table (IRAT), shown in Fig. 3.34. The IRAT tables are located adjacent to the injection tables, just south of the transport-spatial-filter vacuum vessels. The main beam passes sequentially through the IRAT, the injection table, and the transport spatial filter. The alignment beam is injected into the main beam path through the beam combiner on the IRAT and is propagated through the beamline. A series of crosshairs are used to align the beam using video and beam-motion control systems. For the short-pulse beamlines, the alignment beam enters the grating compressor chamber, where

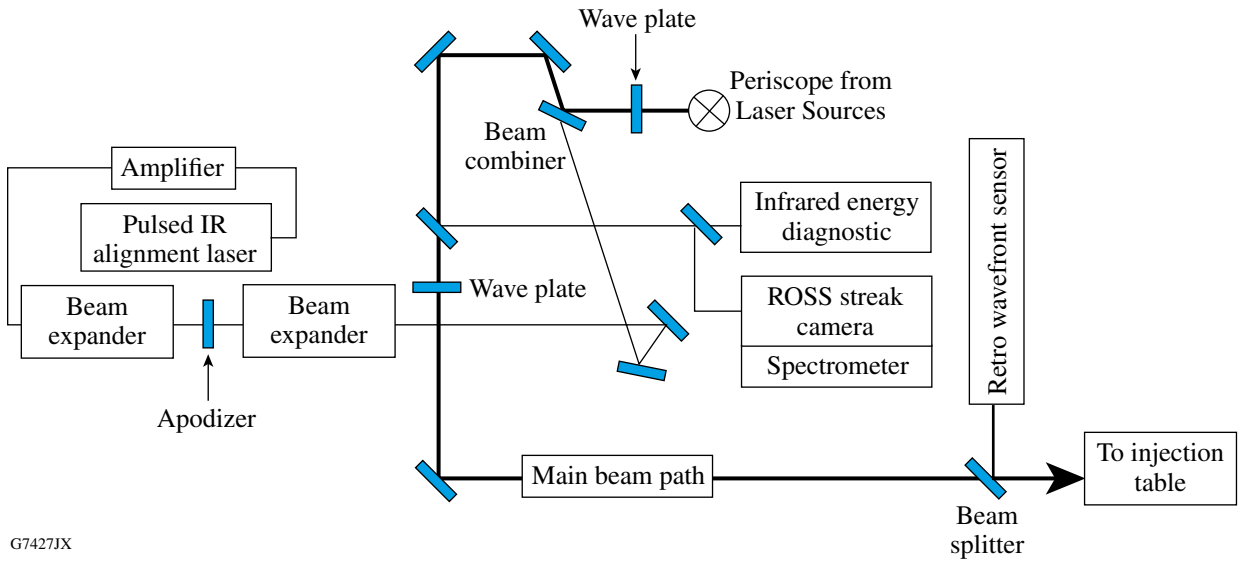

Figure 3.34
Layout of the infrared alignment table. Either the beam from Laser Sources or the IR alignment laser can be selected for injection into the beamline via the injection table.

it traverses either the upper or lower compressor and then to the table containing the short-pulse diagnostics. The IRAT tables also contain a number of diagnostics to measure quantities such as the beam energy, temporal shape, and spectrum.

The beam from the IRAT proceeds to the injection table (Fig. 3.35). A small fraction (0.5%) of the beam is transmitted through a leaky mirror to a number of diagnostics including pointing and centering alignment sensors. The alignment detectors are video-rate CCD cameras that capture pulsed data for analysis with computer software identical to that used on OMEGA. Each of the alignment sensors features low- and high-resolution settings so that both coarse and fine alignment can be electronically sensed. Another portion of the beam is routed to a megapixel scientific (16-bit) near-field camera. A test shot illuminating the system crosshair is captured on this camera. The image is reduced for beam quality as well as alignment prior to executing shots.

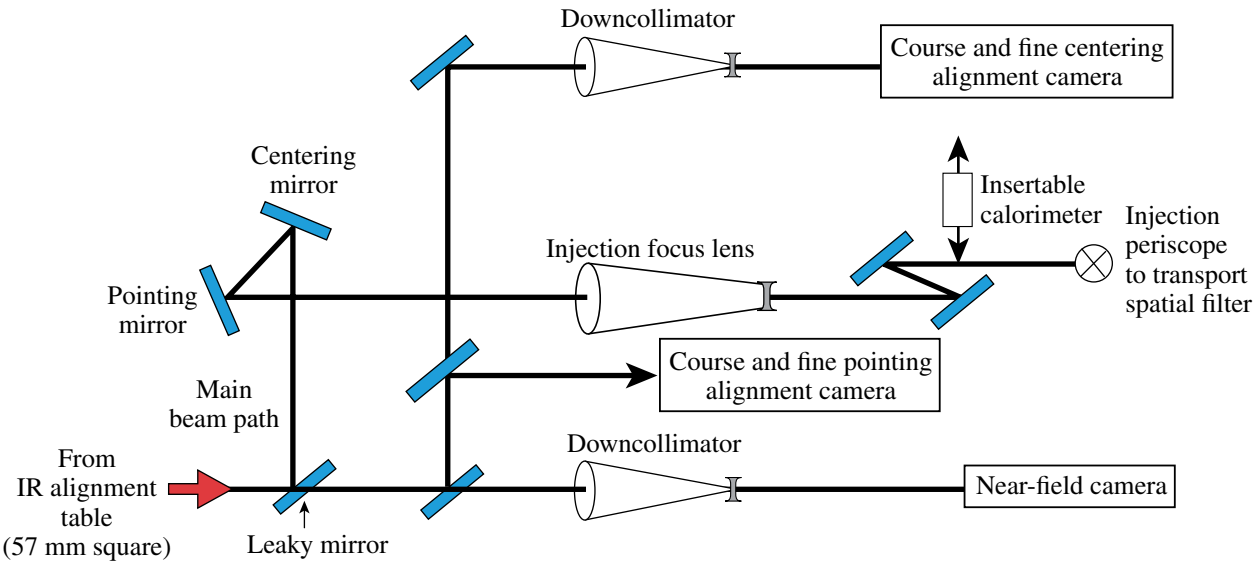

Figure 3.35
Layout of the injection table, indicating the locations of the alignment sensors and the beam path to the transport spatial filter located directly above.

3.5 OPERATIONS

OMEGA EP is operated in the same way as the Omega Laser Facility. The Laser Facility Organization and Regulation Manual[27] addresses critical operations issues and specifies how scientific programs are allocated system time, how system time is scheduled, and how training and safety programs within the facility are conducted. The Omega EP Facility uses a four-volume set of documentation for configuration management and control of operations procedures. Volume VII describes the system architecture, Volume VIII contains all of the written procedures for operations,

Volume IX describes the startup and shutdown procedures, and Volume X addresses the periodic maintenance program. These volumes are available from the "PI Portal" page of the LLE Web site (https://omegaops.lle.rochester.edu/pi_portal.htm).

Execution of effective and safe laser and experimental shots requires a complete and detailed specification of the facility configuration. It includes detailed laser operating parameters, extensive advance planning, and many hours of system preparation prior to and during the actual shot day. The Shot Request Form (SRF) is the primary vehicle for recording and communicating the specifications for a shot. The SRF's are handled identically between laser systems via a common SRF Web page. The SRF enables the requestor to specify whether the shot is an OMEGA, OMEGA EP, or joint system shot.

Supplemental tools and forms are used in planning and communicating the sequences of related shots that are referred to as "campaigns." The SRF is a database object that is created within the LLE computer system primarily via inputs made through a Web-based SRF user interface on the "OMEGA Operations" page of the LLE Web site. This interface consists of a series of pages or screens known as "forms" that collect information of various types. The SRF pages for OMEGA EP include

- General: laser system, PI's, campaign identification, planned date, planned order
- Sources: short/long pulse width, pulse shape, etc.
- Target: characteristics, unique identifier, etc.
- Beams: groups defined by energy, pointing, focus
- Diagnostics: fixed and re-entrant instruments, timing, filtration, alignment, etc.

On the shot day, SRF data values are also accessed directly by the Laser Control System and assist the operators in preparing for and executing the shot. Once an SRF has been used to specify a system shot, it is considered expended and is not reused. The SRF data values are retained in the database indefinitely but may be retrieved for use in data assessment or for the creation of new SRF's.

3.6 REFERENCES

1. J. H. Kelly, L. J. Waxer, V. Bagnoud, I. A. Begishev, J. Bromage, B. E. Kruschwitz, T. J. Kessler, S. J. Loucks, D. N. Maywar, R. L. McCrory, D. D. Meyerhofer, S. F. B. Morse, J. B. Oliver, A. L. Rigatti, A. W. Schmid, C. Stoeckl, S. Dalton, L. Folnsbee, M. J. Guardalben, R. Jungquist, J. Puth, M. J. Shoup III, D. Weiner, and J. D. Zuegel, "OMEGA EP: High-Energy Petawatt Capability for the OMEGA Laser Facility," J. Phys. IV France **133**, 75 (2006).

2. L. J. Waxer, D. N. Maywar, J. H. Kelly, T. J. Kessler, B. E. Kruschwitz, S. J. Loucks, R. L. McCrory, D. D. Meyerhofer, S. F. B. Morse, C. Stoeckl, and J. D. Zuegel, "High-Energy Petawatt Capability for the OMEGA Laser," Opt. Photonics News **16**, 30 (2005).

3. J. Murray, "A Walk Through the National Ignition Facility," *ICF Quarterly Report*, **7**, 95, Lawrence Livermore National Laboratory, Livermore, CA, Report UCRL-LR-105821-97-3 (1997).

4. I. N. Ross, P. Matousek, M. Towrie, A. J. Langley, and J. L. Collier, "The Prospects for Ultrashort Pulse Duration and Ultrahigh Intensity Using Optical Parametric Chirped Pulse Amplifiers," Opt. Commun. **144**, 125 (1997); D. Strickland and G. Mourou, "Compression of Amplified Chirped Optical Pulses," Opt. Commun. **56**, 219 (1985).

5. Time-Bandwidth Products AG (TBP), CH-8005 Zurich, Switzerland.

6. E. B. Treacy, "Optical Pulse Compression with Diffraction Gratings," IEEE J. Quantum Electron. **QE-5**, 454 (1969).

7. J. A. Armstrong, N. Bloembergen, J. Ducuing, and P. S. Pershan, "Interactions Between Light Waves in a Nonlinear Dielectric," Phys. Rev. **127**, 1918 (1962).

8. V. Bagnoud, M. J. Guardalben, J. Puth, J. D. Zuegel, T. Mooney, and P. Dumas, "High-Energy, High-Average-Power Laser with Nd:YLF Rods Corrected by Magnetorheological Finishing," Appl. Opt. **44**, 282 (2005).

9. Koheras A/S, DK-3460 Birkerod, Denmark.

10. M. D. Skeldon, "A High-Bandwidth Electrical Waveform Generator Based on an Aperture-Coupled Stripline," Rev. Sci. Instrum. **71**, 3559 (2000).

11. Kentech Instruments Ltd., South Moreton, Didcot OX11 9AG, Oxfordshire, UK.

12. Spectral Instruments, Tucson, AZ 85745 (http://www.specinst.com/Products/800s_datasheet.pdf).

13. Acton Research Corporation, Acton, MA 01720.

14. Greenfield Technology, Ferme des Arpentis, 91430 Vauhallan, France.

15. C. Dorrer, J. Bromage, and J. D. Zuegel, "High-Dynamic-Range Single-Shot Cross-Correlator Based on an Optical Pulse Replicator," Opt. Express **16**, 13534 (2008).

16. A. DeJager, "Optical Time Domain Reflectometry for the OMEGA EP Laser," *2005 Summer Research Program for High School Juniors at the University of Rochester's Laboratory for Laser Energetics*, University of Rochester, Rochester, NY, LLE Report No. 343 (2006).

17. J. M. McMahon, J. L. Emmett, J. F. Holzrichter, and J. B. Trenholme, "A Glass-Disk-Laser Amplifier," IEEE J. Quantum Electron. **QE-9**, 992 (1973).

18. B. M. Van Wonterghem, J. R. Murray, J. H. Campbell, D. R. Speck, C. E. Barker, I. C. Smith, D. F. Browning, and W. C. Behrendt, "System Description and Initial Performance Results for Beamlet," *ICF Quarterly Report*, **5**, 1, Lawrence Livermore National Laboratory, Livermore, CA, Report UCRL-LR-105821-95-1, NTIS Order No. DE95017171 (1994).

19. E. Grasz, D. Silva, M. McDaniel, D. Tiszauer, A. Rowe, and S. Yakuma, "Transport and Handling," *ICF Annual Report 1997*, Lawrence Livermore National Laboratory, Livermore, CA, Report UCRL-LR-105821-97-3, 214 (1998).

20. LLE's first use of water-cooled flash lamps in a disk amplifier is described in M. J. Lubin, J. M. Soures, and L. M. Goldman, "Large-Aperture Nd:Glass Laser Amplifier for High-Peak-Power Application," J. Appl. Phys. **44**, 347 (1973).

21. The fill factor, f, is defined such that the product of $f\,F_{\text{peak}}$ and the beam aperture equals the integral of the fluence F over the aperture, where F_{peak} is the peak fluence.

22. Richardson Electronics, LaFox, IL 60147-0390.

23. R. A. Zacharias, E. S. Bliss, S. Winters, R. A. Sacks, M. Feldman, A. Grey, J. A. Koch, C. J. Stolz, J. S. Toeppen, L. Van Atta, and B. W. Woods, "Wavefront Control of High-Power Laser Beams in the National Ignition Facility (NIF)," in *Advanced High-Power Lasers*, edited by M. Osinski, H. T. Powell, and K. Toyoda (SPIE, Bellingham, WA, 2000), Vol. 3889, p. 332.

24. R. S. Craxton, "High Efficiency Frequency Tripling Schemes for High Power Nd:Glass Lasers," IEEE J. Quantum Electron. **QE-17**, 1771 (1981).

25. C. E. Barker, B. M. Van Wonterghem, J. M. Auerbach, R. J. Foley, J. R. Murray, J. H. Campbell, J. A. Caird, D. R. Speck, and B. W. Woods, "Design and Performance of the Beamlet Laser Third-Harmonic Frequency Converter," in *First Annual International Conference on Solid State Lasers for Application to Inertial Confinement Fusion*, edited by W. F. Krupke (SPIE, Bellingham, WA, 1995), Vol. 2633, p. 398.

26. P. J. Wegner, J. M. Auerbach, C. E. Barker, S. C. Burkhart, S. A. Couture, J. J. DeYoreo, R. L. Hibbard, L. W. Liou, M. A. Norton, P. A. Whitman, and L. A. Hackel, "Frequency Converter Development for the National Ignition Facility," Lawrence Livermore National Laboratory, Livermore, CA, Report UCRL-JC-129725 (1998).

27. See http://www.lle.rochester.edu/05_omega/05_02_documentation/05_documentation.html.